iScience

CellPress
OPEN ACCESS

Review

Recent advances of two-dimensional materials-based heterostructures for rechargeable batteries

Yinghui Xue,[1,4,*] Tianjie Xu,[1,3,4] Chenyang Wang,[2] and Lei Fu[2,*]

SUMMARY

Because of their unique layer structure, 2D materials have demonstrated to be promising electrode materials for rechargeable batteries. However, individual 2D materials cannot meet all the performance requirements of energy density, power density, and cycle life. Constructing 2D materials-based heterostructures offers an opportunity to synergistically handle the deficiencies of individual 2D materials and modulate the physical and electrochemical properties. The enlarged interlayer distance and increased binding energy with ions of heterostructures can facilitate charge transfer, boost electrochemical reactivities, resulting in an enhanced performance in rechargeable batteries. Here we summarize the latest development of heterostructures consisted of 2D materials and their applications in rechargeable batteries. Firstly, different preparation strategies and optimized structure engineering strategies of 2D materials-based heterostructures are systematically introduced. Secondly, the unique functions of 2D materials-based heterostructures in rechargeable batteries are discussed respectively. Finally, challenges and perspectives are presented to inspire the future study of 2D materials-based heterostructures.

INTRODUCTION

Due to the energy shortage crisis, the transition from traditional energy to renewable energy such as wind energy, solar energy, and tidal energy, is the general trend. However, renewable energy sources cannot be continuously converted into electric energy,[1–4] so energy storage devices are the key to this transition as they can make these intermittent performances continuous and reliable.[5–7] Among energy storage devices, rechargeable batteries (RBs) have advantages of stable performance, long cycle life, and low maintenance, are the best choice for energy storage. Electrode materials play an important role in RBs, and many materials have been proposed as electrode materials.[8] However, the performance achieved at present cannot support the commercial needs, such as the demand for high power density and high energy density.[9–11] High power density can only be achieved in materials where ions and electrons move rapidly, and high energy density requires maximizing charge storage capacity.[12,13] In this regard, 2D materials (2DMs) have open 2D channels that facilitate ions transport and large specific surface area accessible to ions, thereby resulting in fast charge storage and increased capacity. However, individual 2D materials cannot meet all the performance requirements of energy density, power density, and cycle life. For example, graphene shows high electrical conductivity and mechanical strength, but its capacity is limited to a moderate value due to the charge storage on the surface only. Transition metal dichalcogenides (TMDs) exhibit high initial capacities, but suffer from low electrical conductivity and poor capacity retention.

To overcome these limitations, a promising solution may be 2D materials-based heterostructures, which is assembled by different traditional 2D materials.[14–19] When the individual 2D materials layers are assembled into 2D materials-based heterostructures, an enhancement can be achieved by synergistic effect. The application of 2D ionic/electronic conductors can counteract low dynamics of the other material in a heterostructure, thereby improving the overall ion/electron diffusion capability.[14] Due to the weak van der Waals (vdW) force between layers, most 2D heterostructures have large interlayer distance,[20–22] creating a way to not only accommodate larger ions and reduce the energy barriers to ion diffusion, thereby accelerating transportation, but also store larger amounts of ions, leading to higher specific capacity. It is particularly worth mentioning that some heterostructures with normal interlayer distance also present enhanced performance owing to the improved ionic diffusion kinetics.[15] This is attributed to the increase of binding energy between one side of interfaces and ions, which is benifical to the ion accumulation and the reduction of diffusion barriers. Moreover, by defect engineering and interface engineering strategies, it is possible to modulate the physical and chemical properties of 2D materials-based heterostructures, improve theoretical capacities and diffusion kinetics for ions storage, and closely affect the interactions at the interfaces. Besides, 2D materials have high in-plane strength, hence 2D materials-based heterostructures intrinsically have a better ability to accommodate and survive large stresses and strains during ions

[1]Henan Joint International Research Laboratory of Nanocomposite Sensing Materials, Anyang Institute of Technology, Anyang 455000, China
[2]College of Chemistry and Molecular Sciences, Wuhan University, Wuhan 430072, China
[3]Hubei Province Key Laboratory of Science in Metallurgical Process, Wuhan University of Science and Technology, Wuhan 430081, China
[4]These authors contributed equally
*Correspondence: xueyh@ayit.edu.cn (Y.X.), leifu@whu.edu.cn (L.F.)
https://doi.org/10.1016/j.isci.2024.110392

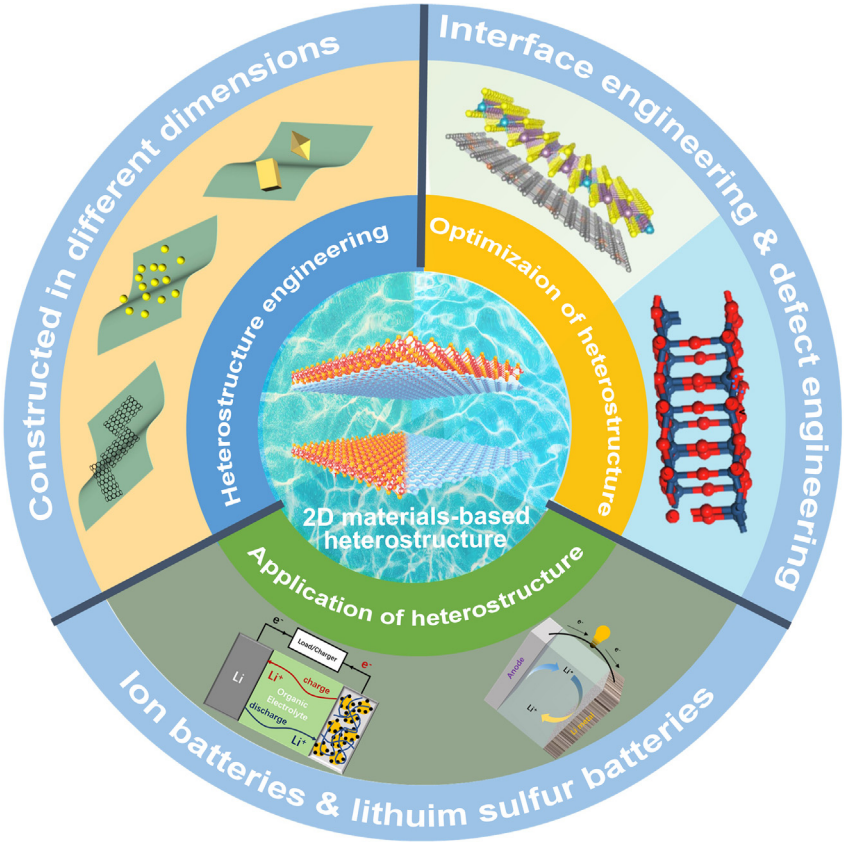

Figure 1. Schematic illustration of 2D materials-based heterostructures and their applications
Reproduced with permission from ref.[23] Copyright 2023 Elsevier B.V. Reproduced with permission from ref.[24] Copyright 2023 Elsevier B.V.

intercalation/deintercalation, so an improved cyclability can be achieved. 2D materials-based heterostructures have been widely used in rechargeable batteries and open unprecedented opportunities for nanoscale design of battery electrodes.

The research of 2D materials-based heterostructures is constantly making new progress, so it is necessary to summarize the latest progress and challenges of 2D materials-based heterostructures for rechargeable batteries, and clarify the future research of 2D materials-based heterostructures. The purpose of this review is to focus on the design engineering of 2D materials-based heterostructures, and latest progress of 2D materials-based heterostructures in rechargeable batteries (Figure 1). It should be noted that most of the 2D materials-based heterostructures here are assembled by vdW force, and in some special cases, there are chemical bonds between 2D materials. Firstly, we introduce the construction of 2D materials-based heterostructures, and the improvement strategy through interface engineering and vacancy defect optimization. Next, we review the recent scientific progress toward the suitability of 2D heterostructures as battery electrodes by first-principles density functional theory-based simulations. Then the advanced functional applications of 2D materials-based heterostructures in alkali ion batteries, zinc ion batteries and lithium sulfur batteries are reviewed. Finally, based on the current research progress, we put forward our personal views on the challenges and future research directions.

HETEROSTRUCTURE ENGINEERING

The vigorous development of 2DMs has also promoted the development of 2D materials-based heterostructures. 2D materials-based heterostructures can be divided into two categories, one is composed of different types of 2DMs to form heterostructures, and the other is mixed-dimensional heterostructures. There is no dangling bond on the surface of the some 2DMs (such as graphene, h-BN, MoS_2), and there is a strong covalent bond in the plane, and the interlayer is combined by a weak vdW force.[25,26] The strong in-plane covalent bond makes the 2D vdW heterojunction have strong in-plane stability, and the relatively weak vdW force is enough to stack the 2D crystal materials together. Therefore, different kinds of 2DMs can be spliced together such as stacking trees to form various types of vdWs heterostructures.[27,28] The mixed-dimensional heterostructure is a heterogeneous interface formed by the combination of 2DMs with zero-dimensional structures (nanoparticles, quantum dots), one-dimensional structures (nanotubes, nanobelts), and three-dimensional structures. Rational design of 2D materials-based heterostructures will improve the physical and chemical properties (Figure 1).

The charge transfer ability of electrode materials is very important for rechargeable batteries. Most two-dimensional electrode materials have high charge transfer kinetics due to their unique planar layered structure. Benefiting from this characteristic, 2DMs and derived heterostructures based on 2DMs show advantages in electrochemical activity and rate capability in rechargeable batteries. The fabrication of 2D materials-based heterostructures electrodes is the biggest challenge in this direction. Although there are many challenges in manufacturing this ideal material frame, the recent success of assembling 2D materials into large-scale heterostructures shows the possibility in this direction. At present, the experimental method for preparing 2D materials-based heterostructure is developed based on the preparation of single-layer 2DMs. In the experiment, a suitable method was used to obtain the single atomic layer, and these individual atomic layers were assembled in the expected stacking order to create the required 2D heterostructure. Similar to the synthesis of individual atomic layers, top-down and bottom-up strategies can be applied to the assembly of 2D materials-based heterostructures. Generally speaking, there are two ways to synthesize heterostructures: mechanical assembly and *in situ* growth. By means of a certain transfer method, the method of placing one 2D material on another 2D material is the mechanical assembly method. This is a common means of constructing heterojunctions. It has the advantages of being simple and direct and conducive to maintaining the lattice structure of 2DMs. As for the *in-situ* growth method, it uses chemical vapor deposition (CVD) or wet chemical synthesis to epitaxially grow another 2D material on the surface of one 2D material. The advantage of the method is that it can better control the shape and structure of the material, and can also more closely combine the lattice between the materials. Since this review focuses on the application of 2D heterostructures in the direction of electrochemical energy storage, we will next introduce the mechanical assembly method and epitaxial growth method around the field of rechargeable batteries.

Mechanical assembly

Mechanical assembly refers to the use of physical means to assemble and stack pre-grown 2D materials in a specified order or angle to form 2D heterostructures, which can avoid lattice mismatch between 2D materials. Mechanical assembly can be divided into solution-based transfer and non-solution-based transfer. Dry transfer refers to the use of van der Waals forces between 2D materials to directly stack different materials together. The more common dry transfer method includes using viscoelastic polydimethylsiloxane (PDMS) membrane as a carrier to transfer two-dimensional materials, and then construct van der Waals heterojunction. The PDMS film with a small amount of 2D material is aligned and contacted with the 2D material on the substrate, then the substrate is heated and the PDMS film is lifted to separate from the 2D material, and the required stacked heterojunction can be quickly obtained. Solution-based transfer is a common method to build a large area of van der Waals heterostructures. The operation process is as follows: first, the prepared 2D material is adhered to the surface of the double-layer viscous polymer medium, and then one layer of polymer is dissolved. The remaining polymer and the attached 2D material are aligned with the target substrate under an optical microscope and placed above the 2D material that needs to be stacked, and slowly move until the 2D materials are bonded together before removing the remaining polymer film layer on the surface of the 2D material. In addition, self-assembly in solution by electrostatic attraction is an extensible method to realize the ordered assembly of heterostructures.[29] For example, Wang et al.[30] reported the direct assembly of chemically exfoliated Cu-HHTP and modified V_2CT_x MXene (MX) nanosheets in a simple solution phase to obtain Cu-HHTP/MX alternately stacked 2D heterostructures. Specifically, a self-assembled Cu-HHTP/MX heterostructure was achieved by electrostatic attraction by mixing a negatively charged Cu-HHTP suspension and a positively charged polydiallyldimethylammonium chloride (PDDA) modified MXene nanosheet suspension in a certain proportion. 2D Cu-HHTP/MX heterostructure establishes an effective charge transfer channel between Cu-HHTP active material and MXene, and MXene nanosheets is helpful to improve the stability of the structure and promote rapid electron transport. Accordingly, the open layered structure of 2D Cu-HHTP/MX heterostructure can provide rapid insertion/removal of Zn^{2+}, thereby achieving enhanced specific capacity and magnification performance. Zhang and colleagues[31] also assembled $Ni(OH)_2$ and PDDA modified graphene oxide (GO) by electrostatic assembly, and then transferred and annealed to construct a 2D rGO/NiO heterostructure film on ITO glass, as shown in Figure 2A. In addition, 2D heterostructures can also be realized by ultrasonic treatment in solution. Xu et al.[32] successfully prepared NiCo-MOF/MXene 2D/2D heterostructures at room temperature by a simple ultrasonic assembly method.

Although wet chemical transfer technology has made some progress in the preparation of electrode materials, there are still some challenges. Firstly, the stacked heterostructure of different 2DMs needs to be combined by electrostatic force, ion charge transfer, hydrogen bonding, covalent bonding and other mechanisms. The requirement of efficient assembly brings limitations, because not all materials will adhere to each other. This means that surface modification is needed to introduce specific functional groups or surfactant molecules, so as to produce certain charge-induced interactions between sheets of different materials. Secondly, the material sheets need to be in face-to-face contact, so that no large gap can be formed in the middle, but at the same time, electrolyte can be allowed to enter.

In situ growth

In-situ growth is another way to construct heterostructures, which can achieve strong and clean interfaces/heterojunctions, because the second material grows directly on the specific crystal plane of the first material. It includes wet chemical synthesis and CVD. Wet chemical synthesis is a common method for *in-situ* construction of 2D heterostructures, which mainly uses hydrothermal or solvothermal reactions. Wet chemical synthesis method has the advantages of high crystallinity, environmental friendliness and good dispersion. Solvothermal method requires sufficient affinity between the template and the precursor of the second material to ensure that the reaction takes place preferentially on the template surface instead of forming individual product particles. Yan's research group[33] prepared a 2D materials-based heterostructure in which SnS_2 nanoplates are vertically anchored to graphene aerogel (SnS_2@GA). Sn^{2+} is immobilized on graphene oxide by coordination with GO surface groups. GO colloidal solution was hydrothermally treated to obtain cylindrical hydrogel (Figure 2B), which ensured that

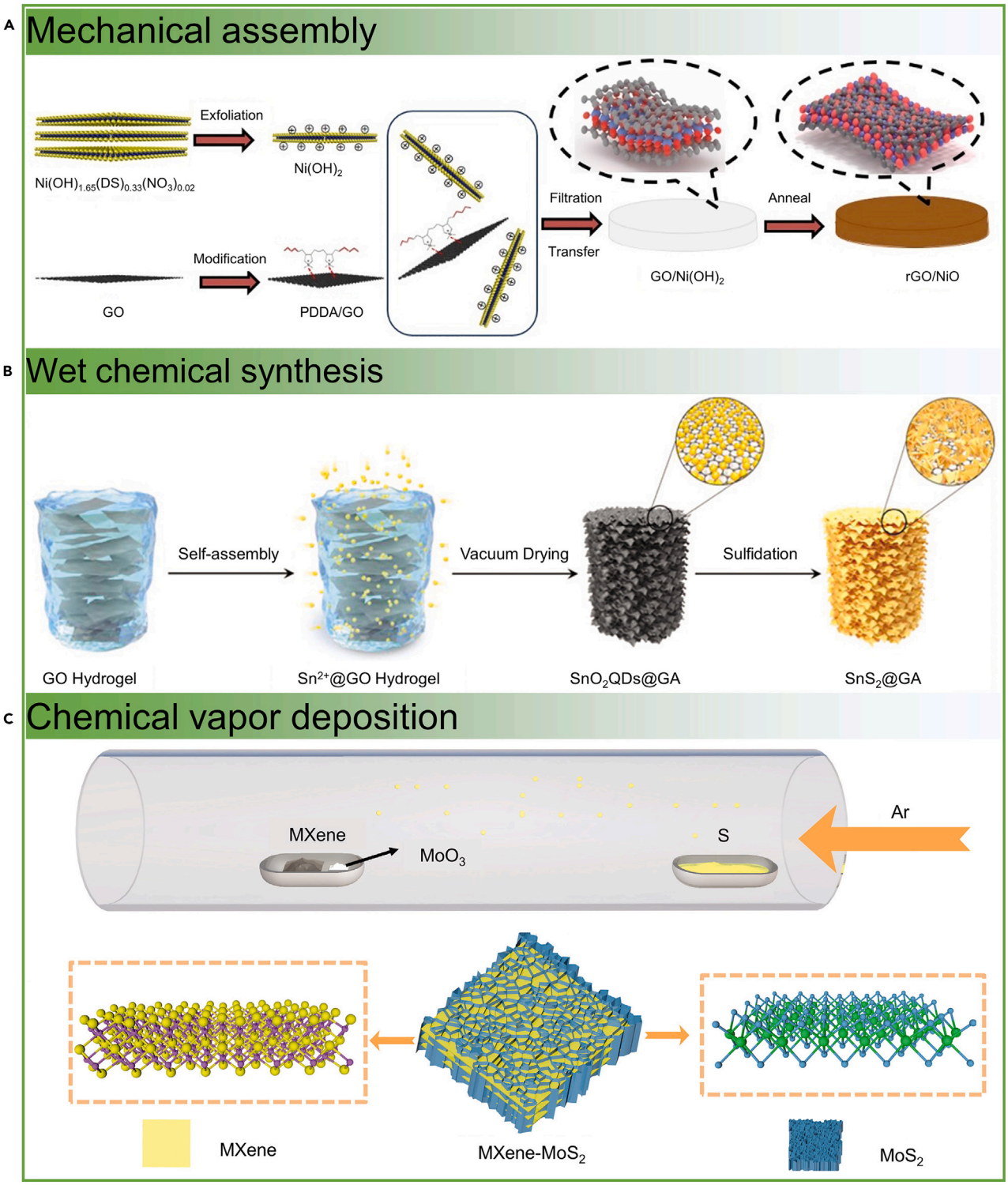

Figure 2. Schematic illustration of assembly of 2D heterostructures

(A) Schematic diagram of the rGO/NiO preparation process. Image A reproduced with permission from ref.[31] Copyright 2021 Elsevier B.V.

(B) Schematic illustration of the synthetic route for preparing SnS_2@GA heterostructures. Image B reproduced with permission from ref.[33] Copyright 2022 Royal Society of Chemistry.

(C) Schematic illustration showing the synthesis process of the MXene-MoS_2 nanocomposites and crystal structure of the corresponding materials. Image C reproduced with permission from ref.[34] Copyright 2023 Springer Nature.

enough surface termination remained on GO surface. When the hydrogel was immersed in $SnCl_2$ aqueous solution with a certain concentration, Sn^{2+} was immobilized on graphene oxide by coordination with GO surface groups, and finally Sn^{2+} nucleated and grew into SnO_2 quantum dots anchored on GA structure. The dense side-to-side heterostructure design significantly increases the active SnS_2 loading in the composites, thus increasing the energy density of the electrodes. In addition, the increase of the number of heterojunction enhances the structural stability of the composites. By combining these characteristics with the advantages of 3D GA, the composite anode exhibits rapid electron and ion migration, excellent structural stability and enhanced pseudocapacitance dominance mechanism. In addition to heterostructures based on graphene, MXene is also commonly used as a growth template to form heterostructures by compounding with other materials. For example, Zhang and his colleagues[35] anchored ZIF-67 on $Ti_3C_2T_x$ MXene nanosheets by *in-situ* growth to form ZIF-67/MXene precursor, and then ZIF-67/MXene was transformed into nitrogen-doped graphite carbon/MXene heterostructure under simple thermal annealing process. Finally, by phosphating, secondary P dopants and micropores were introduced into the skeleton of N-GC/MXene to form graded porous N-P doped graphite carbon/MXene heterostructure.

CVD method is widely used in manufacturing heterostructures, and has the following advantages. In CVD process, 2D heterostructures can be constructed *in situ* in one step, and the size, quality and number of layers can be controlled by adjusting the synthesis conditions. In addition, the number of building blocks can be adjusted to form multiple heterostructures.[36,37] Zhang et al.[34] prepared a stable 2D MXene-MoS_2 heterostructure by CVD. MoO_3 and S powders were selected as the precursors for MoS_2 growth. MoS_2 was formed by the reaction of MoO_3 and S powders at higher temperature. At this time, MXene is also in thermodynamic non-equilibrium state, which can be used as the substrate for MoS_2 growth (Figure 2C). The uniform growth of MoS_2 nanosheets on MXene can prevent the spontaneous oxidation of MXene due to dissolved oxygen, thus ensuring the integrity of MXene structure. In addition, the strong interfacial coupling between highly conductive layered MXene and MoS_2 can achieve rapid charge transfer, which greatly enhances the charge transfer behavior of the electrode.

In general, the above *in-situ* growth method can produce a clean and solid heterogeneous interface, thereby achieving efficient electron transfer and further promoting electrochemical kinetics. However, CVD and wet chemical methods are time-consuming and inefficient. Moreover, the samples may have inevitable damage throughout the process, which hinders them from being suitable for large-scale production of rechargeable battery heterostructure materials.

Optimization of heterostructures

In addition to the above preparation methods, 2D materials-based heterostructures can be further optimized by defect engineering and interface engineering strategies to improve the electrochemical performance and stability. By defect engineering and interface engineering, it is possible to modulate the physical and chemical properties of 2D materials, improve theoretical capacities and diffusion kinetics for ions storage, and closely affect the interactions at the interfaces. Guo et al.[38] used growth covalent bonds to assemble MXene nanosheets and covalent organic frameworks (COF) to construct MXene@COF heterostructure (Figure 3A). Specifically, $Ti_3C_2T_x$ was aminated with NH_2 as the connecting site, and ultra-thin 2D COF-LZU1 was grown on aminated $Ti_3C_2T_x$ nanosheets *in situ* through covalent bonds, resulting in a strong MXene@COF heterostructure with high crystallinity, graded porosity and conductive framework. Xie et al.[24] combined with theoretical calculation to prepare a new interface composed of cobalt doped MoS_2 (Co-MoS_2) and nitrogen doped graphene (NG) in Figure 3B. The designed interfacial doping project significantly improved the Na^+ adsorption capacity, the conductivity of MoS_2 and the electrical transport at the interface during the discharge process. In recent years, defect engineering has been considered as an effective method to modify the surface properties and electronic structure of nanomaterials, and widely used in electrode materials. As an effective strategy, defect engineering can provide new active sites and accelerate ion diffusion for electrode materials. In addition, the presence of defects can increase the surface energy of the system and promote the electrochemical phase transition. Therefore, the effective construction of defects on electrode materials has become a research hotspot in the modification of electrode materials for rechargeable batteries. Oxygen vacancy is an important defect engineering strategy for modifying the surface chemistry and geometry of 2D materials-based heterostructures. For example, Li's group[23] developed VO_2 nanobelts with oxygen vacancies supported on nitrogen-doped carbon nanosheets (VO_{2-x}/NC), as shown in Figure 3C. Nitrogen-doped carbon nanosheets can be used as a 2D growth substrate for VO_2 nanobelt growth and a reducing agent for the formation of oxygen vacancies. The abundant oxygen vacancies provide additional active sites to participate in Na^+ storage. Due to the existence of oxygen vacancies and 2D heterostructures, VO_{2-x}/NC has the characteristics of enhanced conductivity and increased active sites.

APPLICATION IN RECHARGEABLE BATTERIES

Rechargeable batteries, also known as secondary cells, are batteries that can be recharged by driving electric current in the opposite direction of the discharge current. Typical examples are metal ion batteries, lithium-sulfur batteries and metal-air batteries and so on. As mentioned above, 2D materials-based heterostructures have superiorities of high charge transfer kinetics, fast ion diffusion channels, appropriate adhesive capacities to metal ions, huge specific surface area, and enhanced electrochemical reactivity, are promising electrode materials for next-generation rechargeable batteries. In this section, we will discuss some recent progresses in 2D materials-based heterostructures for rechargeable batteries to recount their promising potential in this field.

Theoretical predictions

The variety and quantity of 2D materials are continuously growing, so as the 2D materials-based heterostructures. In order to seek 2D heterostructures for electrode materials more efficiently, theoretical studies on the fundamental design rules of 2D heterostructures for

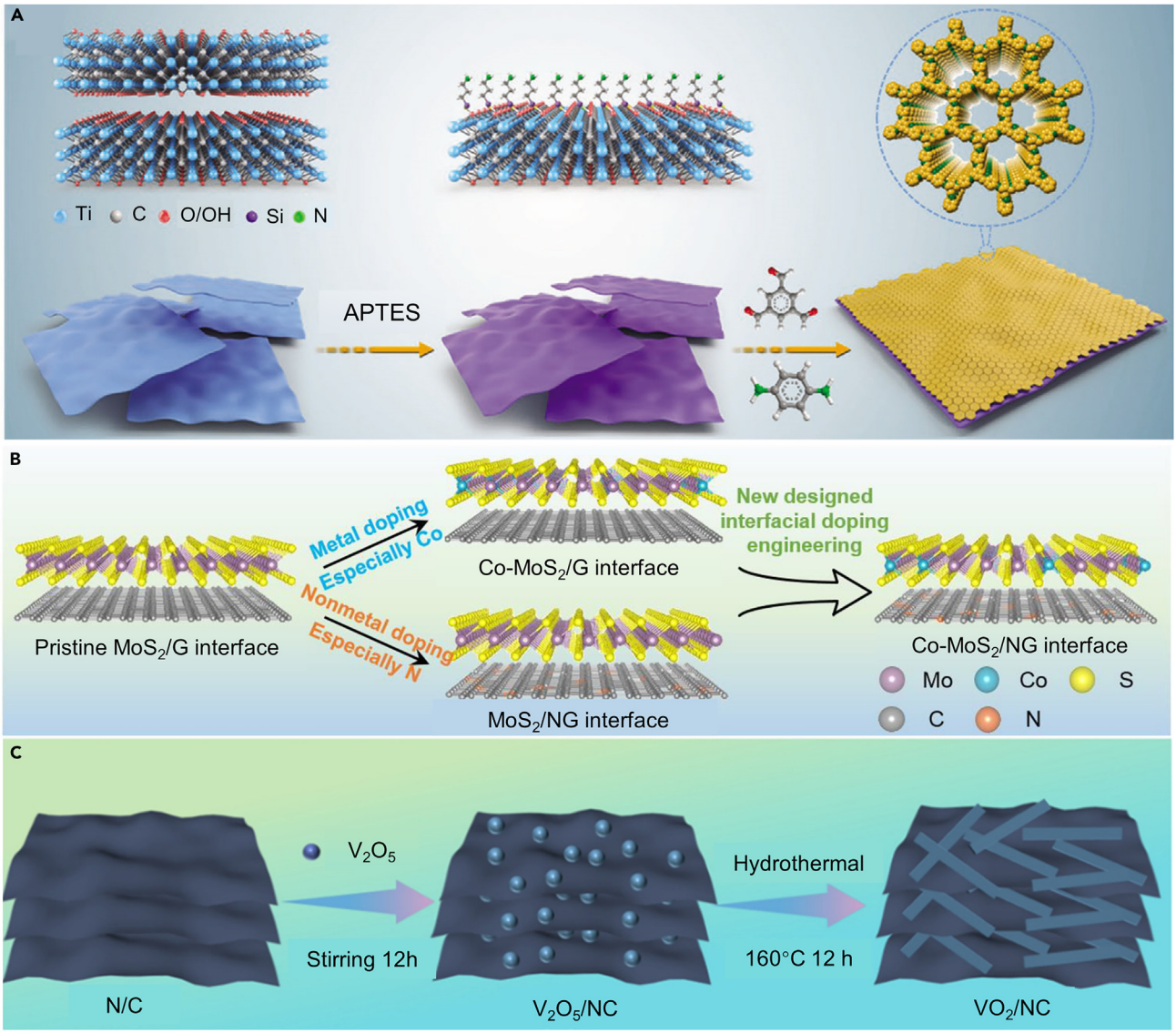

Figure 3. Schematic illustration of optimization of 2D heterostructures

(A) Schematic illustration of MXene covalent amination, followed by MXene@COF-LZU1 growth. Image A reproduced with permission from ref.[38] Copyright 2021 John Wiley and Sons.

(B) Schematic diagram of interfacial doping engineering in MoS_2/G. Image B reproduced with permission from ref.[24] Copyright 2023 Elsevier B.V.

(C) Schematic diagram of the fabrication of VO_{2-x}/NC. Image C reproduced with permission from ref.[23] Copyright 2023 Elsevier B.V.

rechargeable batteries are necessary. Theoretical calculations can explain the thermodynamic stability of 2D heterostructures, and exclude heterostructures that cannot exist stably. Through some key parameters such as specific capacity, open-circuit voltage and even volume expansion for fully lithiated heterostructures, it is possible to judge whether a 2D heterostructure is suitable as electrode materials. Theoretical calculations can also be used to predict the dynamics of ions confined between layers of heterostructures. Furthermore, electrochemical reaction mechanism, ions migration path, and the interfacial electronic structure changes can be clarified by theoretical calculations as well. Here we summarize the recent advances in theoretical calculations of 2D heterostructures for application in rechargeable batteries (Table 1) and illustrate the important role of theoretical calculations in detail with several examples.

Through theoretical calculations, it is possible to determine whether a 2D heterostructure can be used for rechargeable batteries. The monolayers of TiS_2 and MoS_2 may encounter significant limitations when used as stand-alone anode materials in batteries, such as the volume expansion of MoS_2 during metal-ion intercalation[54] and the low energy density of TiS_2 in K-ion batteries.[55] Nair et al.[45] explored the enhanced properties of TiS_2/MoS_2 heterostructures for rechargeable batteries. The calculation results show that the TiS_2/MoS_2 heterostructure possesses good structure stability because of the negative formation energy. Moreover, TiS_2/MoS_2 heterostructures can withstand stresses of

Table 1. Summary of performances of 2D heterostructures as anode materials for rechargeable ion batteries by theoretical calculations

Heterostructure	$E_{formation}$ (eV)	Battery type	E_{bind} (eV)	OCV (V)	$E_{barrier}$ (eV)	Specific capacity (mAh g^{-1})	Reference
Graphene/C_2N	–	Li	−0.12	0.76	0.27	961	Chen et al.[39]
VO_2/VS_2	−0.18	Mg	−4.38	0.55	0.60	301	Luo et al.[40]
VS_2/Ti_2CO_2	–	Na	−2.40	0.21	0.22	601	Song et al.[41]
C_3N/Graphene	−0.62	Li	–	0.40	0.60	558	Gavali et al.[42]
penta-Graphene/penta-BN	−0.12	Li	−0.46	0.93	0.65	1054	Chen et al.[43]
		Na	−0.58	0.74	0.20	1054	
Borophosphene/graphene	−0.21	Li	–	0.70	0.45	427	Gavali and Thapa[44]
TiS_2/MoS_2	−0.49	Li	–	0.68	0.18	100	Nair et al.[45]
		Na	–	0.63	0.07	100	
		K	–	0.74	0.04	100	
Silicene/Boron nitride	−0.72	Na	−1.90	–	0.06	306	Wang et al.[46]
$WS_2/NbSe_2$	–	Li	−3.26	1.52	0.18	842	Liu et al.[47]
Borophosphene/Boron nitride	–	Li	−2.46	1.04	0.35	1698	Khan et al.[48]
MoS_2/N-doped carbon	–	Li	−2.48	–	1.49	815	Zhen et al.[49]
Graphene/MoO_2	0.04	Li	−0.87	1.2	0.07	1411	Ma et al.[50]
Graphene/VS_2	0.69	Li	−1.99	0.65	0.15	771	Liu et al.[51]
		Na	−1.25	0.46	0.08	578	
Graphene/SnS_2	0.12	Li	1.54	–	0.25	586	Samad et al.[52]
		Na	1.36	–	0.13	586	
Graphene/V_2CO_2	−0.02	Li	1.43	1.93	0.60	234	Aierken et al.[53]
Graphene/Ti_2CO_2	−0.02	Li	1.78	1.49	0.30	234	

Note: $E_{formation}$–the formation energy of 2D heterostructures; E_{bind}–the binding energy of metal atom and 2D heterostructures; OCV–the open-circuit voltage of 2D heterostructures with metal; $E_{barrier}$–diffusion barrier energy of ions in 2D heterostructures.

up to 21 GPa and the Young's modulus of the heterostructure is determined to be 142 GPa. Compared with the 2D monolayers of TiS_2 and MoS_2, the heterostructure exhibits stronger alkali Li/Na/K ion adsorption, especially between the layers of the heterogeneous structure due to the strong interlayer interaction. The computed adsorption energies values for Li/Na/K atoms indicate that the site between the Ti atom and the hollow site of MoS_2 is the most favorable site for alkali atoms. The diffusion energy barriers at the bottom layer (outside TiS_2) of heterostructure are significantly lower than those of the monolayers as standalone materials. These findings support TiS_2/MoS_2 heterostructures as attractive flexible anode materials for high-performance alkali-metal ion batteries. Similarly, Gavali et al.[44] concluded that borophosphene and graphene based heterostructures are stable anode materials with high specific capacity. The presence of graphene helps to maintain moderate open-circuit voltage (OCV), low volume expansion, and low Li diffusion barrier energy. Another research by Gavali et al.[42] proposed C_3N/graphene based 2D heterostructure as an efficient anode material for lithium ion batteries (LIBs). The charge transfer of C_3N/graphene depends on the interface and sites of C_3N/graphene, which plays an important role in improving the Li storage capacity, sustaining OCV and maintaining a suitable diffusion barrier. Chen et al.[43] systematically studied the physical properties of the penta-Graphene/penta-BN_2 heterostructure. Results show that the penta-Graphene/penta-BN_2 heterostructure possesses excellent thermodynamic stability and superior conductivity, which provide the prerequisites for its application in Li/Na-ion batteries. In addition to applications in alkali metal ion batteries, $NbSe_2$-graphene 2D heterostructure show potential as a promising anode material for calcium ion battery.[56]

The low diffusion barrier for ions of 2D heterostructures is a key factor to fast charge/discharge rates.[57–59] The explanations of the low barrier focus on the weak adhesion and even energy landscape for ions in the 2D heterostructure.[60] In this theory, it is appropriate for low ion occupancies, but it obviously ignores the Coulomb repulsions between ions at high occupancies. To elucidate the effect of the ion occupancies on the diffusion barrier and further obtain the migration mechanism of ions in a 2D heterostructure, Song et al.[41] performed systematic calculations of VS_2/Ti_2CO_2 heterostructure with different Li intercalation occupancies. According to the traditional individual diffusion mechanism, the diffusion barrier increased from 0.303 to 0.502 eV for Li site occupancy varying from 0.25 to 1, implying that as lithium concentration increases, the diffusivity of lithium decays exponentially. However, the AIMD calculations did not support this trend. The results show that Li diffusivity only decreases approximately linearly with Li vacancy density, and the diffusion barriers are almost constant with occupancy. Further calculations indicate that ions in the heterostructure migrate mainly via a correlation mechanism, and the favorable chemical environments for ions, and large ion spacings during diffusion can ensure a low barrier for various ion occupancies. This

Table 2. Summary of performances of 2D heterostructures as electrode materials for rechargeable ion batteries

Heterostructure	Electrode	Voltange (V)	Capacity (mAh g^{-1})/current density (A g^{-1})	Rate performance (mAh g^{-1})/current density (A g^{-1})	Capacity retention/Cycle number	Reference
V-MXene/V_2O_5	LIB anode	0.01–3	463/0.2	380/5	86%/800 (0.2 A g^{-1})	Dai et al.[67]
aMoO_{3-x}@MXene	LIB anode	0.8–2.8	500/0.2	139/1	–	Yan et al.[68]
Fe_xN@FeOOH	SIB anode	0.01–3	554.8/0.5	89.2/5	–	Guo et al.[69]
SnS_2/graphene	SIB anode	0.01–2.5	690/0.2	492/4	83%/1000 (2 A g^{-1})	Guo et al.[33]
VO_{2-x}/NC	SIB anode	0.01–3	270/0.2	258/10	88.4%/25000 (2 A g^{-1})	Liu et al.[23]
Co-MoS_2/N-doped graphene	SIB anode	0.01–3	415/0.2	327/5	99%/1500 (1 A g^{-1})	Xie et al.[24]
NiS_2/g-C_3N_4/graphene	SIB anode	0.01–3	683/0.1	482/2	100/200 (2 A g^{-1})	Wu et al.[70]
V_2O_5/graphene oxide	ZIB cathode	0.2–1.6	462/0.2	334/5	67.5%/3000 (5 A g^{-1})	Zhang et al.[71]
Cu-HHTP/MXene	ZIB cathode	0.2–1.8	260.1/0.1	173.1/4	92.5%/1000 (5 A g^{-1})	Wang et al.[30]
$H_2V_3O_8$/Mxene	ZIB cathode	0.2–1.6	365/0.2	73/20	–	Liu et al.[72]
V_2O_5/Graphene	ZIB cathode	0.2–1.8	447/0.3	202/30	83%/20000 (30 A g^{-1})	Wang et al.[73]
V_2C/VO_2	LSB cathode	1.6–2.8	813/0.5C	656/5C	–	Xu et al.[74]
mPmPD/MXene	LSB cathode	1.6–2.8	1059.9/0.2C	413/5C	53%/800 (1C)	Xu et al.[75]
$VOPO_4$/graphene	PIB cathode	2.5–4.5	160/0.016	80/3.2	–	Xiong et al.[76]

study provides a new understanding of the high mobility of ions in heterostructures, which is beneficial to the development of 2D material based anodes.

According to Table 1 and the results discussed above, it can be obtained that 2D heterostructures for metal ion storage are conducive to faster ion diffusion and thus have lower diffusion barriers. Based on the bilayer heterostructure model, the enhancement mechanism of graphene-based heterostructure as anode material for ion batteries was demonstrated by theoretical calculation.[61–64] Similarly, the 2D heterostructures we discuss also have these advantages. First, the key characteristic of 2D heterostructures for rechargeable batteries is their charge transport capability. Unique interactions between different layers can modulate the band structure of heterostructures, thereby improving electron transport capabilities. Secondly, the adsorption energy of 2D heterostructures to metal ions is enhanced and the diffusion barrier of ions is reduced compared with that of monolayers. Yu et al.[65] demonstrated a direct relationship between borophene/graphene heterostructure interlayer distance and diffusion barrier through DFT simulations. As the interlayer distance changes from 4 Å to 10 Å, the diffusion barrier decreases from 0.613 eV to 0.353 eV. In addition, 2D heterostructures can also limit volume expansion during metal ion intercalation, which is conducive to cycle stability.[66] Structural changes due to expansion may confine the ion insertion process in a variety of ways confine the ion insertion process. It may lead to the accumulation of insulator products and reduce the capacity of the electrode material. In a word, the role of theoretical calculations are mainly reflected in two aspects, one is to screen promising 2D materials-based heterostructures for rechargeable batteries, and the other is to assist in explaining the mechanism of ions diffusion, charge storage, and desolvation of ions intercalating into the heterostructures and so on.

Functional applications in rechargeable batteries

Recently, heterostructures derived from 2D materials have been widely investigated for rechargeable batteries, due to their tunable size, diversity of interlayer configurations, and adjustable interlayer space. Based on rational molecular and morphology design, 2D heterostructures can be used as electrode materials, lithium hosts, separators, and catalysts.

Electrode materials

2D materials-based heterostructures have large interfacial contact area and multiple 2D channels, which lead to large mass-transfer and charge storage. Because of the interaction at the heterointerfaces of 2D nanosheets, some new properties such as robust electronic and ionic conductivities can be generated, resulting in an enhanced charge storage capacity. The Table 2 summarizes the application of 2D heterostructures in rechargeable batteries.

Dai et al.[67] designed a freestanding electrode consisting of vertically aligned 2D materials-based heterostructures (V-MXene/V_2O_5). The vertically aligned 2D materials-based heterostructures can facilitate electron transport, accommodate the volume expansion and provide vertical channels affording pathways for rapid electron/ion transport over the entire electrode. This design offers several advantages that enhance the cycling stability and electrochemical kinetics and therefore superior energy storage performance. The self-supporting V-MXene/V_2O_5 membrane electrode containing 40 wt % V_2O_5 retained a cycle stability of 358 mAh g^{-1} after 1000 charge-discharge cycles at 5 A g^{-1}. At a current density of 0.2 A g^{-1}, the electrodes with 1 and 5 mg cm^{-2} of V-MXene/V_2O_5 deliver 472 and 300 mAh g^{-1}, respectively.

In the pursuit of high-performance energy storage materials, 2D materials-based heterostructures offer an excellent option. However, there exists a performance ceiling, limited by their vdW interactions. The vdW 2D heterostructures may suffer from poor cyclability as the repeated intercalation of Li ions within the vdW space causes dissociation of the heterostructures.[77] So Yan et al.[68] designed a facile synthesis route to etch Al out of MAX phase using *in-situ* formed HCl, and prepared 2D amorphous MoO_{3-x}@MXene non-vdW heterostructures (Figure 4A). Due to the formation of $MoOCl_3$ in the etch reaction, MoO^{3+} cations could be embedded into the MXene layers and increase the interspacing of MXenes, which would transform to a layer of molybdenum oxides on the surface of MXenes to form amorphous MoO_{3-x}@MXene heterostructures after the thermal treatment. High resolution transmission electron microscope (HRTEM) image in Figure 4B demonstrates two distinct regions on the same nanosheet, a crystalline phase that can be assigned to Ti_3C_2-type MXene phase and an amorphous phase can be assigned to amorphous MoO_{3-x}. Scanning TEM-EDX mapping in Figure 4C shows the even distribution of Ti, C, Mo and O, which confirms the formation of amorphous MoO_{3-x}@MXene heterostructures. X-ray photoelectron spectroscopy (XPS) analysis and Fourier transform infrared spectrometer (FTIR) spectra support the presence of Ti−O−Mo covalent bonds in amorphous MoO_{3-x}@MXene heterostructures. As shown in Figure 4D, after 500 cycles at 200 mA g^{-1}, the capacity of amorphous MoO_{3-x}@MXene heterostructures remains about 500 C g^{-1}. Even at a high rate of 1000 mA g^{-1} (Figure 4E), the electrode still delivers 500 C g^{-1}. DFT calculations reveal enhanced conductivity and 2D Li^+ diffusion. Figure 4F shows the charge density difference of the non-vdW heterostructure model to see that the Ti atoms on the conductive MXene nanosheets provide a large number of electrons to the broken MoO_3 layer through the Ti-O-Mo covalent bond, which means that the conductivity of the broken MoO_3 layer is improved compared to the MXene nanosheets below. The restacked 2D non-vdW heterostructure can simultaneously exist surface-controlled interlayer diffusion and diffusion-controlled intralayer diffusion (Figure 4G), which optimizes the kinetics of lithium ion storage when realizing the full utilization of amorphous MoO_{3-x} layer. The storage of lithium ions exceeding its theoretical capacity provides theoretical guidance for us to rationally design amorphous materials to adjust the kinetics of Li^+ diffusion in other active materials of LIBs.

Sodium ion batteries (SIBs) are promising supplements to LIBs in certain applications such like short-range electric vehicles, grid energy storage and special equipment because of the abundant sodium resources and low cost. However, the insertion of larger Na ions into the host materials may lead to sluggish diffusion kinetics and poor structural stability of the electrode caused by the distortions in the host lattice during the cycling process.[79] The 2D materials-based heterostructures exhibit a series of superiorities such as great acceleration of ion conduction,[60] significant interface effect with improved electronic conductivity and strong ionic adsorption that can promote the electrochemical reaction kinetics,[80] and strong in-plane effect and ultrathin structure leading to excellent mechanical strength.[81] With the above consensus, some progresses have been made in the application of 2D materials-based heterostructures in SIBs recently.[23,24,33,69,70,78,82]

Yu et al.[78] share similar views with the aforementioned Yan et al.[68] that amorphous materials have unique advantages of faster diffusion kinetics, larger free volume, and multiple active sites. So, Yu et al. devised a methodology to rationally fabricate a unique 2D heterostructure composed of amorphous MoS_3-on-reduced graphene oxide (MoS_3-on-rGO) surface through an isotropy growth mechanism. As shown in Figures 4H–4J, the amorphous MoS_3 gradually covered the graphene surface, indicating an isotropic growth process. The adsorption energy of Na on graphene-supported MoS_3 is comparatively lower than that on crystalline MoS_2 and amorphous MoS_3 (Figure 4K), indicating enhanced adsorption capacity and faster storage kinetics of Na in amorphous structures, and further suggesting the presence of the interface effect. Moreover, the amorphous MoS_3-on-rGO exhibits negligible volume expansion during the intercalation of sodium, which is ascribed to the disordered nanostructure of the amorphous MoS_3-on-rGO with abundant defect and internal free volume. As expected, the amorphous MoS_3-on-rGO shows higher reversible capacity, better cyclic stability (Figure 4L), and superior rate performance. The $Na_3V_2(PO_4)_3$//MoS_3-on-rGO sodium-ion full cell can still deliver 336 mAh g^{-1} even after 350 cycles at a current density of 2.0 A g^{-1} (Figure 4M). Furthermore, the amorphous MoS_3-on-rGO also performs excellently in solid-state sodium ion batteries, potassium-ion batteries, zinc-ion batteries, and hybrid supercapacitors, demonstrating its promising application prospect. As described earlier, interfacial doping engineering has been considered a promising strategy to regulate the properties of 2D materials-based heterostructures, which is also applied to improve the reaction kinetics of 2D heterostructures in SIBs.

As a more abundant and safer alternative to LIBs, aqueous rechargeable zinc-ion batteries (ZIBs) using water-based electrolytes hold great potential in grid energy storage.[83] The significant advantage of ZIBs is that metallic zinc anodes possess a low redox potential and good compatibility with water and can in principle provide a high capacity (820 mAh g^{-1}) because of multiple electron transfer.[84] But zinc metal anodes suffer from dendrite issues and side reactions, thus restricting their practical application. Engineering zinc anodes by introducing the 2D materials are widely investigated to alleviate these issues.[85,86] However, the application of 2D heterostructures in zinc anodes is very rare and remains to be further developed. On the cathode side, V_2O_5 crystal with open layered structure attracted more attention because the highest theoretical Zn^{2+} storage capacity, low-cost and easy production.[87] However, crystal V_2O_5 cathodes suffer from the slow diffusion of divalent Zn^{2+}, which is related to their strong electrostatic interaction with the host materials, and unsatisfactory structural stability during the insertion/extraction of Zn^{2+}.[88] Utilizing amorphous V_2O_5 as a host material is a feasible solution to the sluggish reaction kinetics. Wang et al.[73] reported a 2D template ion adsorption method for the assembling of amorphous V_2O_5/graphene (A-V_2O_5/G) 2D heterostructures with strong-coupling effect. The amorphous V_2O_5 layer has the advantages of numerous active sites and minimal volume change. Figure 5A shows dense characteristics of the alternative graphene and amorphous V_2O_5 in 2D heterostructure. Besides, HRTEM image and selected area electron diffraction (SAED) image in Figure 5B indicate the uniform amorphous V_2O_5 closely anchored onto graphene. When assembled in ZIBs, A-V_2O_5/G cathode disclosed average discharge capacities of 404, 352, 306, 289, 259, 222, and 202 mAh g^{-1} at the current densities of 0.5, 1, 3, 5, 10, 20, and 30 A g^{-1} (Figure 5C). After 20,000 cycles, A-V_2O_5/G exhibited ultra-long cycling stability with a capacity retention of ~83% (Figure 5D). Zhang et al.[71] also designed a 2D heterostructure combining amorphous V_2O_5 and graphene oxide,

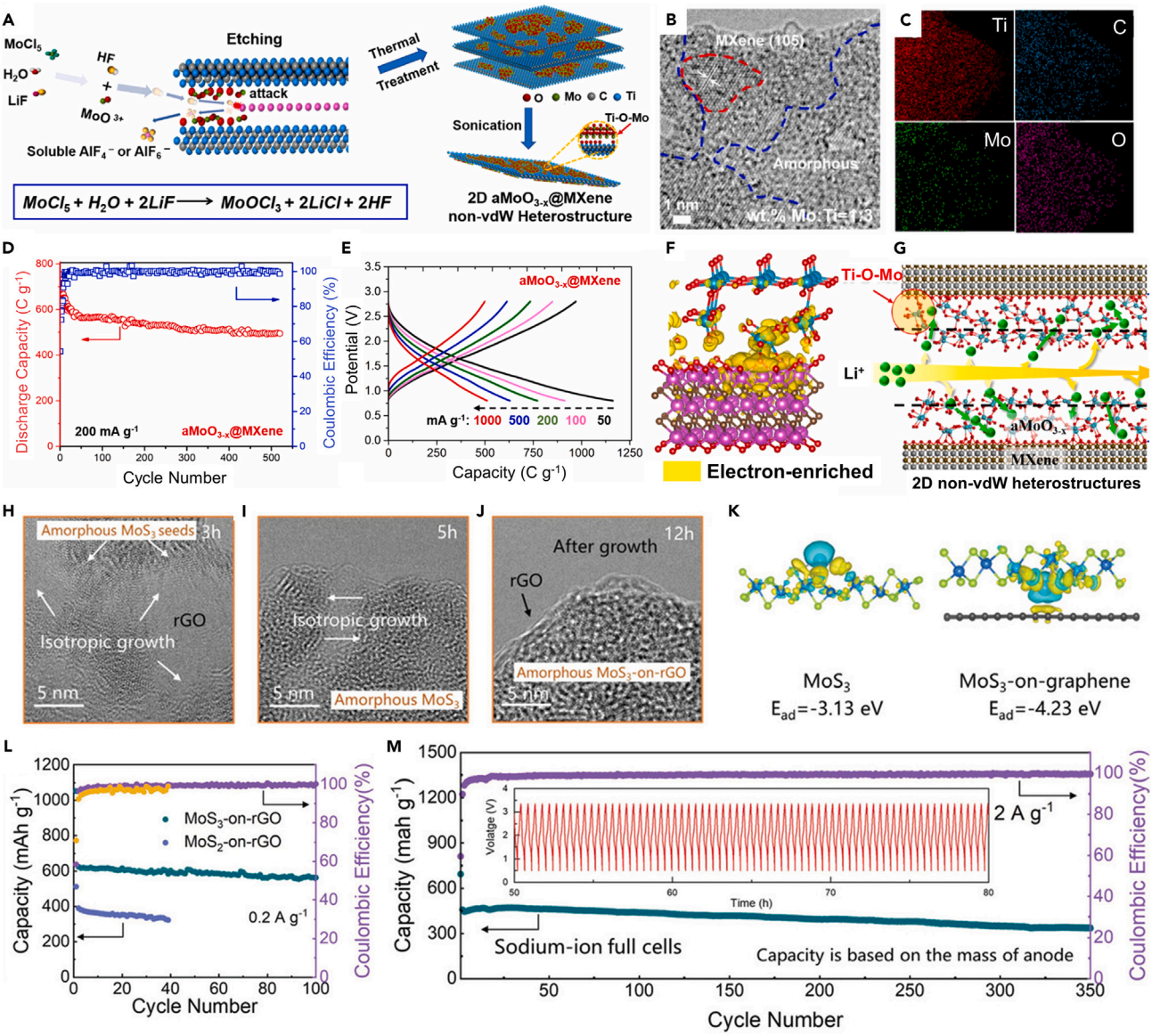

Figure 4. 2D heterostructure for lithium storage and sodium storage

(A) Materials characterization of 2D MoO_{3-x}@MXene non-vdW heterostructures.

(B) HRTEM images of 2D heterostructures (Mo:Ti weight ratio of 1:3) with a crystalline area circled by a red dotted line and an amorphous area circled by blue dotted lines.

(C) STEM-EDX mappings of Ti, C, Mo and O from a 2D heterostructure (Mo:Ti weight ratio of 1:3).

(D) Cycling performance of $aMoO_{3-x}$@MXene non-vdW heterostructures at 200 mA g^{-1}.

(E) Charge-discharge curves at different rates for $aMoO_{3-x}$@MXene non-vdW heterostructures.

(F) Difference charge density of MoO_3@$Ti_3C_2O_{2-x}$(III) heterostructure with a formation of Ti−O−Mo covalent bond. Yellow means gaining electrons and the isovalue is 0.0015.

(G) Illustration of facile capacitor-like interlayer diffusion and diffusion-controlled intralayer diffusion. Images A−G reproduced with permission from ref.[68] Copyright 2021 Elsevier B.V.

(H−J) Isotropic growth process of amorphous MoS_3 from seeds to 2D structure at 3, 5, and 12 h.

(K) Na adsorption models and corresponding adsorption energies in amorphous MoS_3 and amorphous MoS_3/graphene heterointerface, respectively.

(L) Cycle performance of MoS_3-on-rGO and crystal MoS_2-on-rGO for SIB at 0.2 A g^{-1}.

(M) Long cycle performance of SIFC at 2.0 A g^{-1}. Images H−M reproduced with permission from ref.[78] Copyright 2021 Elsevier B.V.

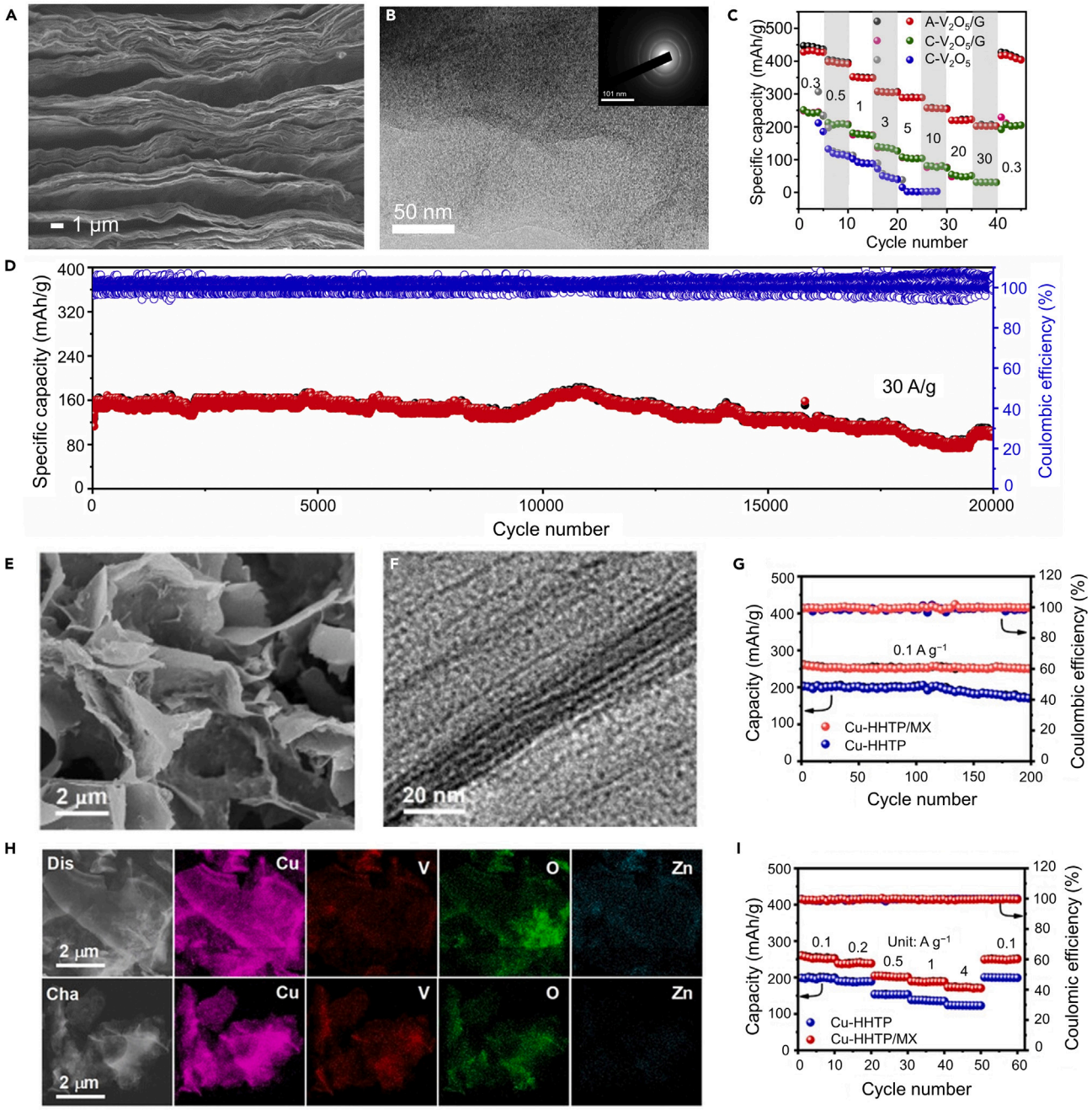

Figure 5. The application of 2D heterostructures in ZIBs

(A and B) Cross-section SEM images, HRTEM image and SAED pattern (inset) of A-V_2O_5/G heterostructures.

(C) Rate capability of A-V_2O_5/G-ZIBs, obtained from 0.3 to 30 A g^{-1}.

(D) Long-term cyclability of A-V_2O_5/G-ZIBs tested at a high current density of 30 A g^{-1} for 20,000 cycles. Images A–D reproduced with permission from ref.[73] Copyright 2020 Elsevier B.V.

(E and F) SEM and HRTEM images of Cu-HHTP/MX.

(G) Electrochemical performances of Cu-HHTP/MX.

(H) HAADF-STEM and the corresponding elemental mapping images recorded at the fully discharged and charged states.

(I) Rate capabilities of the Cu-HHTP and Cu-HHTP/MX. Images E–I reproduced with permission from ref.[30] Copyright 2023 John Wiley and Sons.

and achieved scale production by spray drying technique. In addition to V_2O_5, 2D MOFs can also be used as the cathodes for high-performance ZIBs due to their large one-dimensional channels. But the intrinsic poor electrical conductivity and low structural stability hinder their advances.[89] Wang et al.[30] incorporated chemically exfoliated Cu-HHTP and modified V_2CT_x MXene nanosheets via the facile solution-phase direct assembly to construct a 2D heterostructure. In this structure, MXene nanosheets not only improve the conductivity but also prevent the aggregation of Cu-HHTP during the repeated charge-discharge cycles, while Cu-HHTP layers can act as the main active layer for Zn^{2+} storage and also as a spacer layer to isolate the MXene nanosheets. SEM image of Cu-HHTP/MXene in Figure 5E show a 3D architecture composed of crumpled thin layers. And HRTEM image (Figure 5F) reveal that the thin layers possess multilayer structures consisting of stacked nanosheets. The reversible storage of Zn^{2+} ions in the Cu-HHTP/MXene heterostructure is confirmed by ex situ XRD and ex situ XPS, which is consistent with the result of high-angle annular dark field-scanning transmission electron microscopy (HAADF-STEM) and the corresponding elemental mapping images (Figure 5H). The Cu-HHTP/MXene delivers s a reversible specific capacity of 260.1 mAh g^{-1} and stable cycling performance after 200 cycles at 0.1 A g^{-1} (Figure 5G). Even at a maximum current density of 4 A g^{-1}, the Cu-HHTP/MXene can achieve the reversible capacity of 170.6 mAh g^{-1} (Figure 5I). The excellent electrochemical performance is ascribed to good structural stability, high electrical conductivity and faster Zn^{2+} diffusion kinetics.

Lithium hosts

In addition to being used as electrode materials, 2D materials-based heterostructures can also be lithium hosts in Li metal batteries. As reported by Guo et al.,[38] MXene nanosheets are covalently assembled with COF to extend the chemical space of 2D heterostructures. Ultrathin 2D COF-LZU1 can grow *in situ* on amine-modified $Ti_3C_2T_x$ nanosheets by covalent bonding, creating a stable MXene@COF heterostructure with high crystallinity, hierarchical porosity, and conductive frameworks. The thickness increased to approximately 13 nm after the growth of COF (Figure 6B). HRTEM image of the MXene@COF in Figure 6A shows the interplanar lattice spacing of MXene (1.3 nm). The elemental mapping images (Figure 6C) show the uniform and compact growth of COF on MXene nanosheets. The lithium nucleation overpotential of MXene@COF heterostructure is 13 mV, which is far less than that of Cu electrode, suggesting a kinetically favorable nucleation process on MXene@COF. A reasonable explanation for this phenomenon is that the Li-N interactions could generate homogeneous Li^+ distributions within all COF channels and, therefore, promote uniform Li nucleation. As shown in Figures 6D and 6E, after 50 cycles at 3 mA cm^{-2}, Li deposition within the MXene@COF scaffold was compact and dendrite-free. The MXene@COF host was electroplated with a Li areal capacity of ≈10 mAh cm^{-2}, followed by galvanostatic tests at 3 mA cm^{-2} over 800 h (Figure 6F), which exhibited improved CE and long cycling stability. When tested in full cell, Li/MXene@COF anodes also delivered promising cyclability with $LiFePO_4$ and sulfur (CNT-S) cathodes (Figures 6G and 6H).

Separators

Owing to the remarkably high energy density endowed by multi-electron conversion reaction, lithium sulfur batteries are considered as one of the most promising next-generation energy storage systems.[90] However, the polysulfide shuttling seriously hinders the application.[91,92] 2D materials-based heterostructures can not only enables rapid electron/ion transport kinetics, but also expose rich active sites to propel the adsorption and conversion of lithium polysulfide, effectively suppress the shuttle effect.[93] Recently 2D heterostructures made some breakthroughs in commercial separator modification. Long et al.[94] developed a 2D heterostructure interlayer with montmorillonite (MMT) monolayers uniformly distributed on RGO by electrostatic assembly (Figure 7A). TEM image in Figure 7B clearly shows the sheet-like morphology of MMT/RGO without significant stacking and aggregation, which can expose more active sites for the polysulfide conversion. The fully exposed Si-OH groups on MMT impart the heterostructure with good affinity to polysulfides through Lewis acid-based interaction and promote the fast ion transport due to the low barrier of ion diffusion. The RGO can provide instant electron conduction pathways for the as-adsorbed polysulfides, ensuring rapid electrochemical redox reaction kinetics. After 45 cycles at 1 C, the Li anode with MMT/RGO-modified separators (MMT/RGO-PP) exhibits a smooth surface (Figure 7C). As shown in Figure 7D, the battery with MMT/RGO-PP also exhibits higher peak current density and narrower peak separation than those with RGO-PP, MMT-PP, and pristine PP, indicating the lowest electrochemical polarization achieved by the MMT/RGO heterostructure. The battery with MMT/RGO-PP delivers a high capacity of 1398 mAh g^{-1} at 0.1C, excellent rate performance of 848 mAh g^{-1} even at 3 C (Figure 7E), and low capacity decay rates of 0.011% per cycle at 1C over 200 cycles (Figure 7F).

Another research about separator modification is the 2D MXene-MOF ($Ti_3C_2T_x$-CoBDC) heterostructure reported by Mai et al.[95] A bottom-up synthesis strategy is utilized for the preparation of $Ti_3C_2T_x$-CoBDC nanosheets, wherein the $Ti_3C_2T_x$ nanosheets serve as the synthetic template for the *in-situ* deposition of CoBDC (Figure 8A). The HRTEM picture of the 2D heterostructure nanosheets in Figure 8B reveals that CoBDC is evenly distributed on $Ti_3C_2T_x$. The successful assembly of $Ti_3C_2T_x$-CoBDC heterostructure was further demonstrated in XRD pattern (Figure 8C). Within this 2D heterostructure, CoBDC exhibits a pronounced capacity for adsorbing polysulfides, while $Ti_3C_2T_x$ demonstrates superior catalytic prowess toward polysulfides, alongside commendable electrical conductivity, thereby expediting the conversion of intercepted polysulfides. The cell with $Ti_3C_2T_x$-CoBDC@PP separators has a discharge specific capacity of 1255 mAh g^{-1} at 0.5C and 82% capacity retention after 100 cycles (Figure 8D), as well as a high rate capability of 654 mAh g^{-1} even at 3C (Figure 8E).

Catalysts

Rechargeable lithium-oxygen batteries (LOBs) are considered a replacement for LIBs due to their high theoretical energy density of 3505 Wh kg^{-1} and operating voltage of 2.96 V. Due to the low conductivity and slow reaction kinetics of the fully discharged product Li_2O_2, catalysts are needed to promote the electrode reaction.[41,96,97] Gong et al.[98] prepared $MoS_2/ZnIn_2S_4$ heterostructure nanosheet arrays using a simple

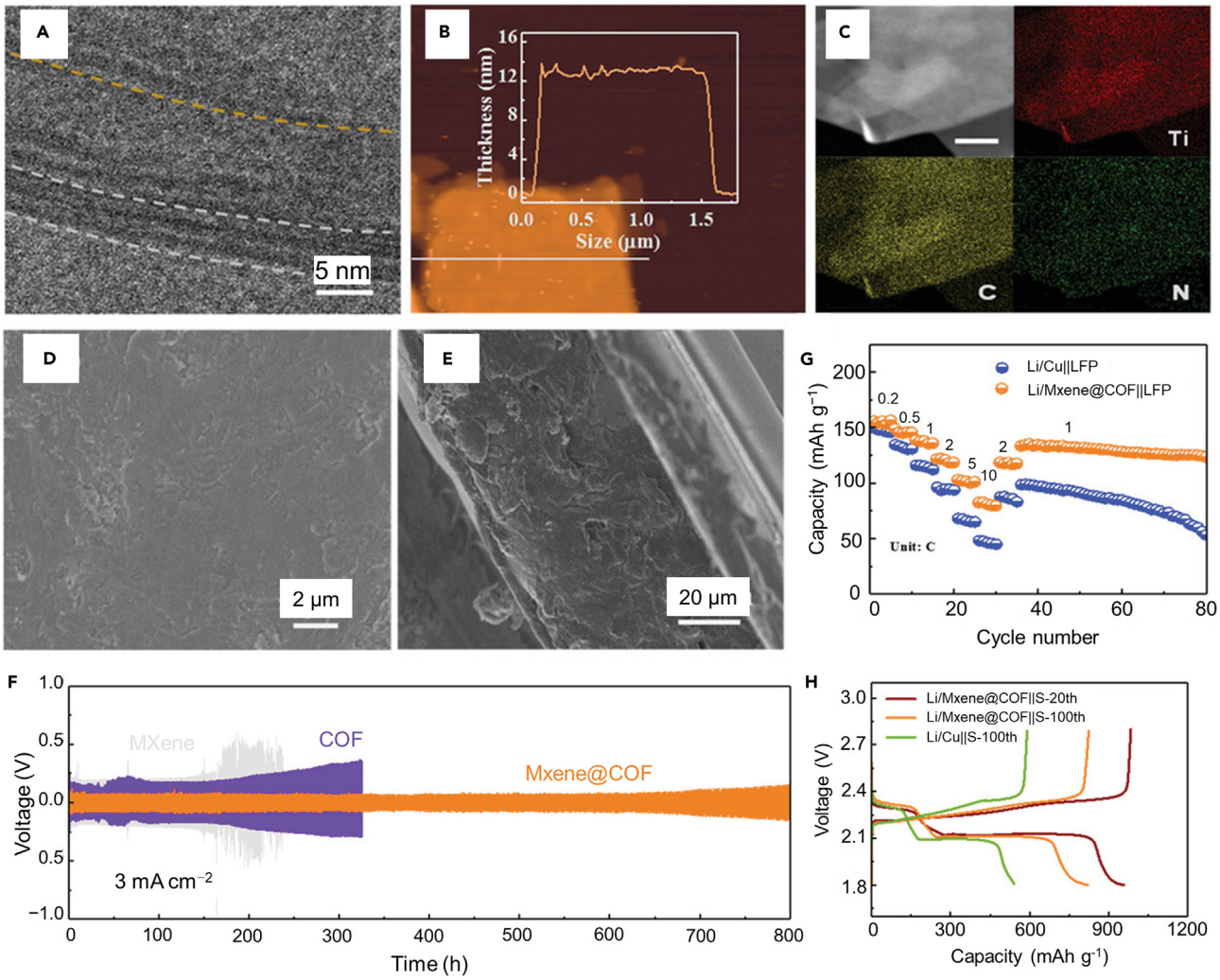

Figure 6. Schematical illustration of the MXene@COF heterostructure for lithium hosts

(A) HRTEM images of MXene@COF nanosheets.

(B and C) AFM image and EDS mapping images (scale bar: 100 nm) of MXene@COF nanosheets.

(D and E) Li deposition morphologies after 50 plating/stripping cycles for MXene@COF electrodes.

(F) Cycling voltage profiles of symmetric cells at 3 mA cm^{-2}.

(G) Rate performance of Li/Cu||LFP full cell.

(H) Discharge/charge curves of Li/MXene@COF||S at 0.5 C. Images A–H reproduced with permission from ref.[38] Copyright 2021 John Wiley and Sons.

solvothermal method, and tight 2D nanojunctions can accelerate charge transfer within the heterostructure interface. The assembled battery delivers a high discharge potential of 3.18 V and a low charge potential of 3.29 V, resulting in an extremely narrow overpotential of 110 mV and high energy efficiency of 96.7%. Construction of the $MoS_2/ZnIn_2S_4$ heterostructure can enhance the generation, separation and transport of photogenerated electrons and holes, thus promoting oxygen reduction reaction (ORR) and oxygen evolution reaction (OER) during discharge/charging. In addition, Xin et al.[99] prepared CoNi/MoC heterostructures as catalysts for zinc-air batteries. The heterostructures shows the positive half-wave potential of 0.89 V (vs. RHE) and small Tafel slope of 51.1 mV dec^{-1} for ORR, coupled by the enhanced OER performance with an overpotential of 335 mV at 10 mA cm^{-2}.

SUMMARY

We review the design, synthesis, and most prominent applications of 2D materials-based heterostructures in rechargeable batteries. Unique 2D materials-based heterostructures have been designed by mechanical assembly and *in-situ* growth methods, and many lateral heterostructures and heterostructure interfaces have been realized. In addition, the different configurations of 2D materials-based heterostructures also enrich their structural diversity, including the interface of van der Waals interaction and non-van der Waals interaction, and the

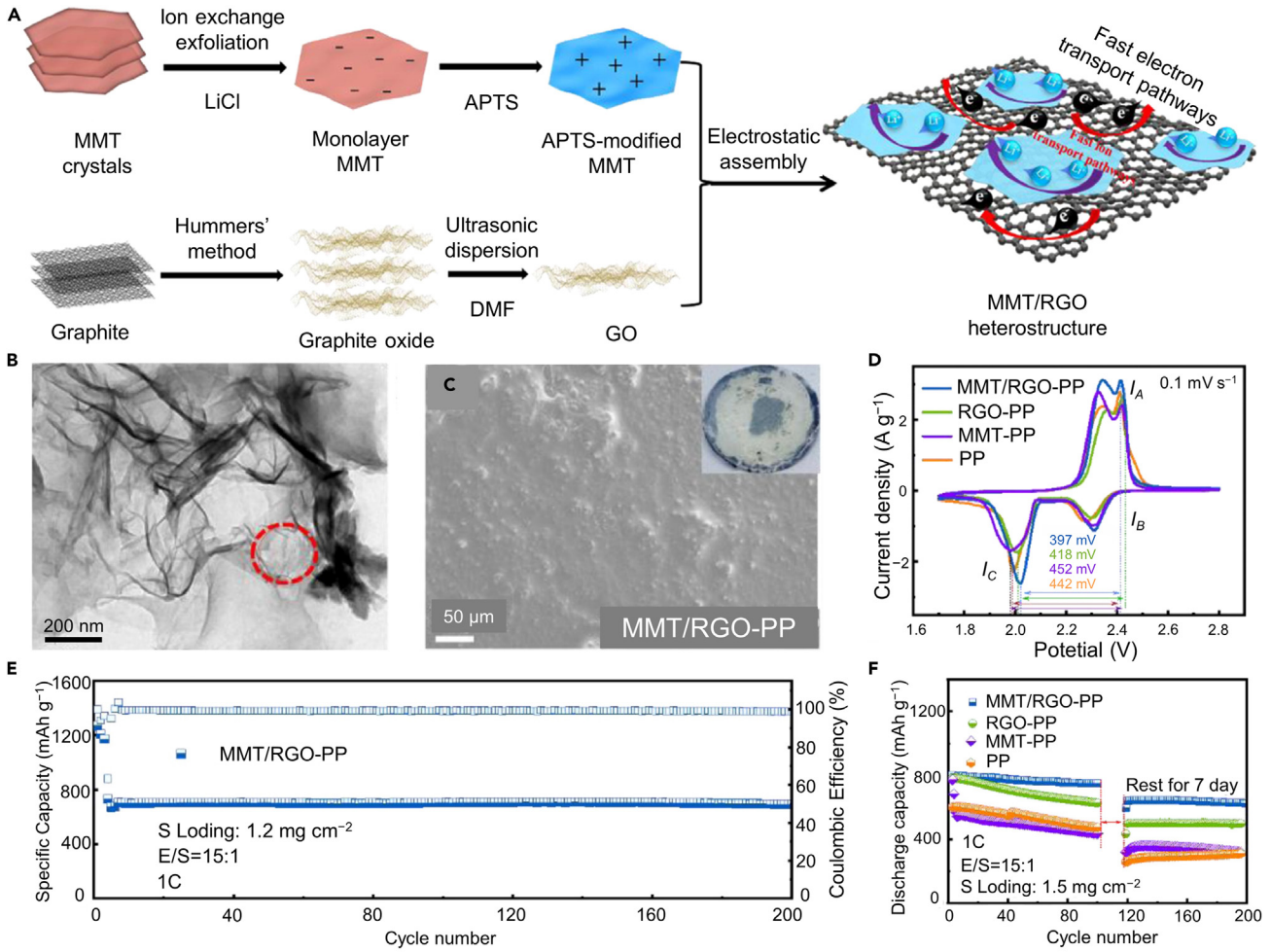

Figure 7. Schematical illustration of the preparation of the MMT/RGO 2D heterostructure separators for lithium-sulfur batteries

(A) Schematical illustration of the preparation of the MMT/RGO 2D heterostructure.

(B) TEM image of MMT/RGO.

(C) SEM images of the lithium metal anode surfaces from the Li-S batteries using MMT/RGO-PP after 45 cycles at 1 C. Inset: digital photos of the separators in the cycled batteries.

(D) CV curves of the Li-S batteries with various separators at a scan rate of 0.1 mV s^{-1}.

(E) Cycling stability at 1 C with a sulfur loading of 1.2 mg cm^{-2}.

(F) Cycling performance of the Li-S batteries using MMT/RGO-PP, RGO-PP, MMT-PP and PP at 1 C containing an interruption rest for 7 days. Images A–F reproduced with permission from ref.[94] Copyright 2022 Elsevier B.V.

heterostructures formed by 2DMs and other dimensional materials. The unique 2D heterostructure has a large surface area and abundant active sites, which improves the performance of the battery when used as an electrode material for rechargeable batteries. Researchers continue to further develop functional 2D materials-based heterostructures through advanced experimental techniques and theoretical calculations to meet the needs of rechargeable batteries for power density and cycle stability. However, some challenges related to the preparation and application of 2D materials-based heterostructures still need to be solved.

1) The first is the low product rate of the method for preparing 2D materials-based heterostructures. Mechanical assembly usually requires the interaction of individual components to form heterostructures, such as the introduction of surface modification to induce charge. However, the introduction of surfactants will lead to interfacial contamination and low product yield. The *in-situ* growth method can form a clean and solid interface, but it requires good lattice matching or additional induction force and other prerequisites, which hinders their wide application in ion batteries. The rational design of synthesis method is still necessary to improve the quality of the 2D materials-based heterostructures.
2) The exact function and reaction kinetics of 2D heterostructures in electrochemical reactions need to be elucidated. Most of the existing studies believe that the synergistic effect of heterostructures enhances their activity in electrochemical reactions. However, the exact

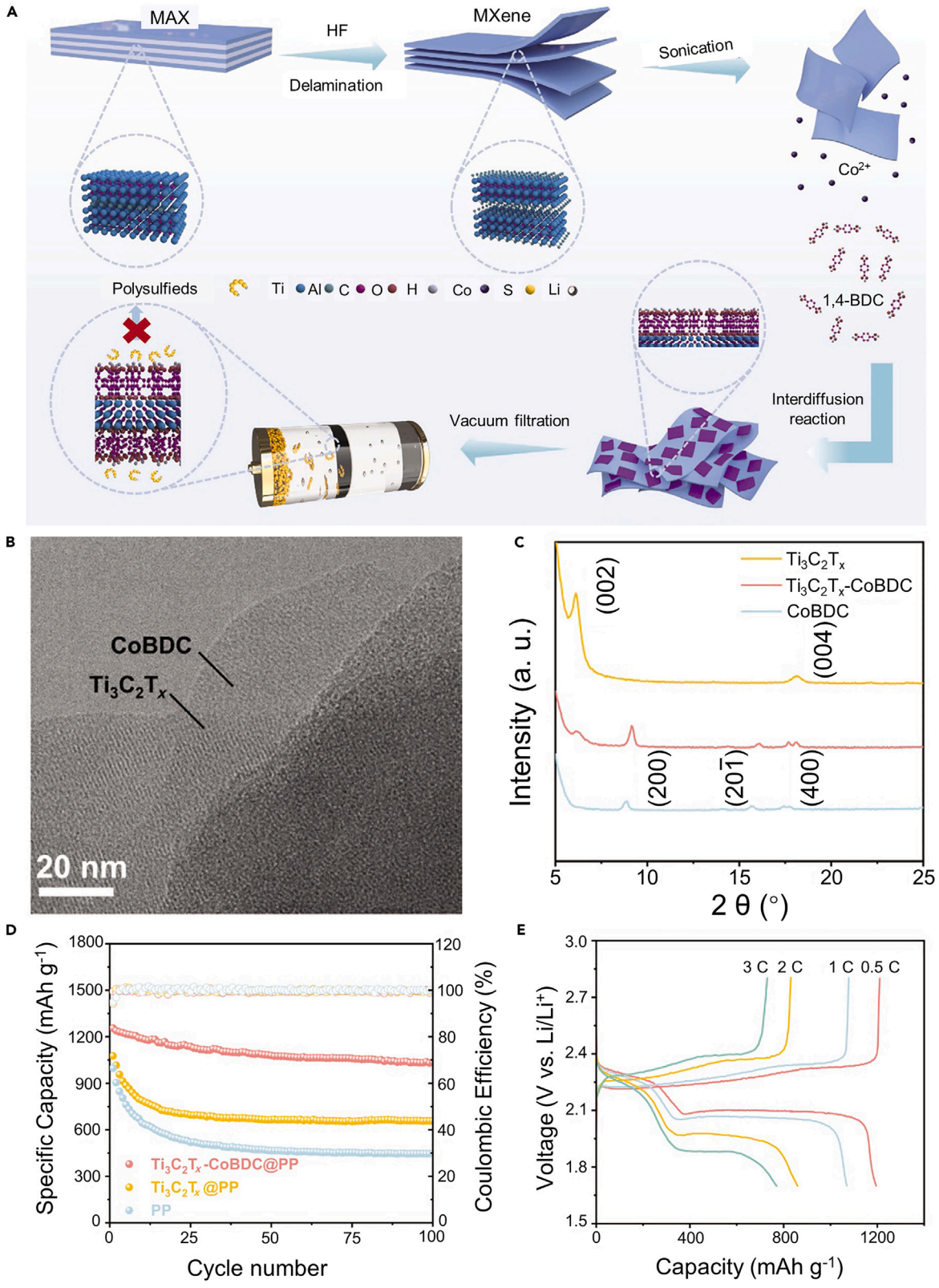
A
MAX
HF
Delamination
MXene
Sonication
Co2+
1,4-BDC
Polysulfieds
Ti Al C O H Co S Li
Interdiffusion reaction
Vacuum filtration
B
CoBDC
Ti3C2Tx
20 nm
C
Ti3C2Tx
Ti3C2Tx-CoBDC
CoBDC
(002)
(004)
(200)
(20$\bar{1}$)
(400)
Intensity (a. u.)
2 θ (°)
D
Specific Capacity (mAh g-1)
Coulombic Efficiency (%)
Ti3C2Tx-CoBDC@PP
Ti3C2Tx @PP
PP
Cycle number
E
3 C 2 C 1 C 0.5 C
Voltage (V vs. Li/Li+)
Capacity (mAh g-1)

Figure 8. Schematical illustration of the methods of the $Ti_3C_2T_x$-CoBDC@PP separator for lithium-sulfur batteries

(A) Synthesis process illustration of $Ti_3C_2T_x$-CoBDC, and its working mechanism in lithium-sulfur battery.

(B) HRTEM image of $Ti_3C_2T_x$-CoBDC.

(C) XRD patterns of the $Ti_3C_2T_x$, $Ti_3C_2T_x$-CoBDC and CoBDC.

(D) Electrochemical performance of the Li-S cells with different separators at 0.5 C.

(E) Galvanostatic charge-discharge profiles of the Li-S cell with $Ti_3C_2T_x$-CoBDC@PP separator at different rates. Images A–E reproduced with permission from ref.[95] Copyright 2023 Springer Nature.

reaction kinetics is still unclear. It is necessary to observe and simulate the reaction mechanism and dynamics of heterostructures in the electrochemical process by means of advanced *in-situ* characterization techniques combined with theoretical calculations, so as to provide experimental and theoretical guidance for the subsequent design of specific heterostructures.

3) The configuration of the heterostructure also affects the electrochemical performance. Different configurations will affect the characteristics of the heterogeneous interface. However, there is a lack of understanding of the stable heterostructure configuration of electrode materials in theory and experiment. The novel structure configuration can be simulated by the DFT calculation method.

ACKNOWLEDGMENTS

This work was supported by the National Natural Science Foundation of China (Grant 22025303), the Science and Technology Project of Henan Province (Grant 242102240085) and the Postgraduate Education Reform and Quality Improvement Project of Henan Province (No.YJS2023JD60).

AUTHOR CONTRIBUTIONS

L.F., and Y.H.X. conceived the idea and designed the frame. Y.H.X. and T.J.X. wrote the first draft of the article. All authors commented, edited, and revised the final article.

DECLARATION OF INTERESTS

The authors declare no conflicts of interest.

REFERENCES

1. Larcher, D., and Tarascon, J.M. (2015). Towards greener and more sustainable batteries for electrical energy storage. Nat. Chem. *7*, 19–29. https://doi.org/10.1038/nchem.2085.
2. Ponraj, J.S., Narayanan, M.V., Dharman, R.K., Santiyagu, V., Gopal, R., and Gaspar, J. (2021). Recent advances and need of green synthesis in two-dimensional materials for energy conversion and storage applications. Curr. Nanosci. *17*, 554–571. https://doi.org/10.2174/1573413716999210101122503.
3. Mendil, M., De Domenico, A., Heiries, V., Caire, R., and Hadjsaid, N. (2017). Battery aging-aware energy management of green small cells powered by the smart grid. EURASIP J. Wirel. Commun. Netw. *2017*, 127. https://doi.org/10.1186/s13638-017-0913-4.
4. Jin, C., Nai, J., Sheng, O., Yuan, H., Zhang, W., Tao, X., and Lou, X.W. (2021). Biomass-based materials for green lithium secondary batteries. Energy Environ. Sci. *14*, 1326–1379. https://doi.org/10.1039/d0ee02848g.
5. Mahlia, T.M.I., Saktisandan, T.J., Jannifar, A., Hasan, M.H., and Matseelar, H.S.C. (2014). A review of available methods and development on energy storage; technology update. Renew. Sustain. Energy Rev. *33*, 532–545. https://doi.org/10.1016/j.rser.2014.01.068.
6. Koohi-Fayegh, S., and Rosen, M.A. (2020). A review of energy storage types, applications and recent developments. J. Energy Storage *27*, 101047. https://doi.org/10.1016/j.est.2019.101047.
7. Xue, Y., Zhang, Q., Wang, W., Cao, H., Yang, Q., and Fu, L. (2017). Opening two-dimensional materials for energy conversion and storage: A concept. Adv. Energy Mater. *7*, 1602684. https://doi.org/10.1002/aenm.201602684.
8. Xu, T., Wang, Y., Xue, Y., Li, J., and Wang, Y. (2023). MXenes@metal-organic framework hybrids for energy storage and electrocatalytic application: Insights into recent advances. Chem. Eng. J. *470*, 144247. https://doi.org/10.1016/j.cej.2023.144247.
9. Nayak, P.K., Yang, L., Brehm, W., and Adelhelm, P. (2018). From lithium-ion to sodium-ion batteries: Advantages, challenges, and surprises. Angew. Chem. Int. Ed. *57*, 102–120. https://doi.org/10.1002/anie.201703772.
10. Ma, H., Zhang, H., and Xue, M. (2021). Research progress and practical challenges of aqueous sodium-ion batteries. Acta Chimi. Sin. *79*, 388–405. https://doi.org/10.6023/a20100492.
11. Zhang, L., Li, X., Yang, M., and Chen, W. (2021). High-safety separators for lithium-ion batteries and sodium-ion batteries: Advances and perspective. Energy Stor. Mater. *41*, 522–545. https://doi.org/10.1016/j.ensm.2021.06.033.
12. Sarycheva, A., Polemi, A., Liu, Y., Dandekar, K., Anasori, B., and Gogotsi, Y. (2018). 2D titanium carbide (MXene) for wireless communication. Sci. Adv. *4*, eaau0920. https://doi.org/10.1126/sciadv.aau0920.
13. Alarcon-Angeles, G., Palomar-Pardave, M., and Merkoci, A. (2018). 2D materials-based platforms for electroanalysis applications. Electroanalysis *30*, 1271–1280. https://doi.org/10.1002/elan.201800245.
14. Fan, F.R., Wang, R., Zhang, H., and Wu, W. (2021). Emerging beyond-graphene elemental 2D materials for energy and catalysis applications. Chem. Soc. Rev. *50*, 10983–11031. https://doi.org/10.1039/c9cs00821g.
15. Wang, Y., Guo, T., Alhajji, E., Tian, Z., Shi, Z., Zhang, Y.-Z., and Alshareef, H.N. (2022). MXenes for sulfur-based batteries. Adv. Energy Mater. *13*, 2202860. https://doi.org/10.1002/aenm.202202860.
16. Xu, T., Wang, Y., Xiong, Z., Wang, Y., Zhou, Y., and Li, X. (2022). A rising 2D star: Novel MBenes with excellent performance in energy conversion and storage. Nano-Micro Lett. *15*, 6. https://doi.org/10.1007/s40820-022-00976-5.
17. Liu, Y., Xu, X., Shao, Z., and Jiang, S.P. (2020). Metal-organic frameworks derived porous carbon, metal oxides and metal sulfides-based compounds for supercapacitors application. Energy Stor. Mater. *26*, 1–22. https://doi.org/10.1016/j.ensm.2019.12.019.
18. Dharmalingam, P., Palani, G., Apsari, R., Kannan, K., Lakkaboyana, S.K., Venkateswarlu, K., Kumar, V., and Ali, Y. (2022). Synthesis of metal oxides/sulfides-based nanocomposites and their environmental applications: A review. Mater. Today Sustain. *20*, 100232. https://doi.org/10.1016/j.mtsust.2022.100232.
19. Min, Y., Im, E., Hwang, G.-T., Kim, J.-W., Ahn, C.-W., Choi, J.-J., Hahn, B.-D., Choi, J.-H., Yoon, W.-H., Park, D.-S., et al. (2019). Heterostructures in two-dimensional colloidal metal chalcogenides: Synthetic fundamentals and applications. Nano Res. *12*, 1750–1769. https://doi.org/10.1007/s12274-019-2432-6.

20. Xiang, R., Inoue, T., Zheng, Y., Kumamoto, A., Qian, Y., Sato, Y., Liu, M., Tang, D., Gokhale, D., Guo, J., et al. (2020). One-dimensional van der Waals heterostructures. Science *367*, 537–542. https://doi.org/10.1126/science.aaz2570.
21. Wu, Y., Zhang, S., Zhang, J., Wang, W., Zhu, Y.L., Hu, J., Yin, G., Wong, K., Fang, C., Wan, C., et al. (2020). Neel-type skyrmion in WTe_2/Fe_3GeTe_2 van der Waals heterostructure. Nat. Commun. *11*, 3860. https://doi.org/10.1038/s41467-020-17566-x.
22. Frisenda, R., Navarro-Moratalla, E., Gant, P., Perez De Lara, D., Jarillo-Herrero, P., Gorbachev, R.V., and Castellanos-Gomez, A. (2018). Recent progress in the assembly of nanodevices and van der Waals heterostructures by deterministic placement of 2D materials. Chem. Soc. Rev. *47*, 53–68. https://doi.org/10.1039/c7cs00556c.
23. Liu, B., Zhang, H., Yuan, C., Geng, Q., Li, Y., Hu, J., Lu, Z., Xie, J., Hao, A., and Cao, Y. (2023). Construction of oxygen vacancies and heterostructure in VO_{2-x}/NC with enhanced reversible capacity, accelerated redox kinetics, and stable cycling life for sodium ion storage. J. Colloid Interface Sci. *646*, 34–42. https://doi.org/10.1016/j.jcis.2023.05.047.
24. Xie, H., Chen, B., Liu, C., Wu, G., Sui, S., Liu, E., Zhou, G., He, C., Hu, W., and Zhao, N. (2023). Engineering the interfacial doping of 2D heterostructures with good bidirectional reaction kinetics for durably reversible sodium-ion batteries. Energy Stor. Mater. *60*, 102830. https://doi.org/10.1016/j.ensm.2023.102830.
25. Wang, S., Zhao, S., Guo, X., and Wang, G. (2021). 2D Material-Based Heterostructures for Rechargeable Batteries. Adv. Energy Mater. *12*, 2100864. https://doi.org/10.1002/aenm.202100864.
26. Hu, Z., Liu, Q., Chou, S.-L., and Dou, S.-X. (2021). Two-dimensional material-based heterostructures for rechargeable batteries. Cell Rep. Phys. Sci. *2*, 100286. https://doi.org/10.1016/j.xcrp.2020.100286.
27. Zhou, J., Xin, K., Zhao, X., Li, D., Wei, Z., and Xia, J. (2022). Recent progress in optoelectronic applications of hybrid 2D/3D silicon-based heterostructures. Sci. China Mater. *65*, 876–895. https://doi.org/10.1007/s40843-021-1939-0.
28. Liu, Y., Zhang, S., He, J., Wang, Z.M., and Liu, Z. (2019). Recent progress in the fabrication, properties, and devices of heterostructures based on 2d materials. Nano-Micro Lett. *11*, 13. https://doi.org/10.1007/s40820-019-0245-5.
29. Feng, D., Li, X., Zhang, L., and Qiao, Z.-A. (2023). Self-assembly method for two-dimensional mesoporous materials: A review for recent progress. Chem. Synth. *3*, 37. https://doi.org/10.20517/cs.2023.26.
30. Wang, Y., Song, J., and Wong, W.-Y. (2023). Constructing 2D sandwich-like MOF/MXene heterostructures for durable and fast aqueous zinc-ion batteries. Angew. Chem. Int. Ed. *62*, e202218343. https://doi.org/10.1002/anie.202218343.
31. Xue, J., Xu, H., Wang, S., Hao, T., Yang, Y., Zhang, X., Song, Y., Li, Y., and Zhao, J. (2021). Design and synthesis of 2D rGO/NiO heterostructure composites for high-performance electrochromic energy storage. Appl. Surf. Sci. *565*, 150512. https://doi.org/10.1016/j.apsusc.2021.150512.
32. Xu, D., Zhang, Z., Tao, K., and Han, L. (2023). A heterostructure of a 2D bimetallic metal-organic framework assembled on an MXene for high-performance supercapacitors. Dalton Trans. *52*, 2455–2462. https://doi.org/10.1039/d2dt03872b.
33. Guo, X., Wang, S., Yu, L., Guo, C., Yan, P., Gao, H., and Liu, H. (2022). Dense SnS_2 nanoplates vertically anchored on a graphene aerogel for pseudocapacitive sodium storage. Mater. Chem. Front. *6*, 325–332. https://doi.org/10.1039/d1qm01369f.
34. Zhang, R., Sun, Y., Jiao, F., Li, L., Geng, D., and Hu, W. (2023). MXene-MoS_2 nanocomposites via chemical vapor deposition with enhanced electrocatalytic activity for hydrogen evolution. Nano Res. *16*, 8937–8944. https://doi.org/10.1007/s12274-023-5602-5.
35. Zhang, Y., Li, H., Yang, Q., Zhang, S., Zhao, B., Wu, J., Shang, N., Zhao, X., Xiao, Z., Zang, X., et al. (2023). Core-shell 2D nanoarchitectures: Engineering N, P-doped graphitic carbon/MXene heterostructures for superior capacitive deionization. J. Mater. Chem. A *11*, 14356–14365. https://doi.org/10.1039/d3ta00696d.
36. Gong, Y., Lin, J., Wang, X., Shi, G., Lei, S., Lin, Z., Zou, X., Ye, G., Vajtai, R., Yakobson, B.I., et al. (2014). Vertical and in-plane heterostructures from WS_2/MoS_2 monolayers. Nat. Mater. *13*, 1135–1142. https://doi.org/10.1038/nmat4091.
37. Dong, S., Zhang, X., Nathamgari, S.S.P., Krayev, A., Zhang, X., Hwang, J.W., Ajayan, P.M., and Espinosa, H.D. (2022). Facile fabrication of 2D material multilayers and vdW heterostructures with multimodal microscopy and AFM characterization. Mater. Today *52*, 31–42. https://doi.org/10.1016/j.mattod.2022.01.002.
38. Guo, D., Ming, F., Shinde, D.B., Cao, L., Huang, G., Li, C., Li, Z., Yuan, Y., Hedhili, M.N., Alshareef, H.N., and Lai, Z. (2021). Covalent assembly of two-dimensional COF-on-MXene heterostructures enables fast charging lithium hosts. Adv. Funct. Mater. *31*, 2101194. https://doi.org/10.1002/adfm.202101194.
39. Chen, Y.W., Wang, Q.R., Zhang, Q., Zhang, S.L., and Zhang, Y. (2023). Graphene/C_2N lateral heterostructures as promising anode materials for lithium-ion batteries. Phys. Chem. Chem. Phys. *25*, 26557–26565. https://doi.org/10.1039/d3cp03295g.
40. Luo, L., Tan, S., Gao, Z., Yang, X., Xu, J., Huang, G., Wang, J., and Pan, F. (2023). A two-dimensional VO_2/VS_2 heterostructure as a promising cathode material for rechargeable Mg batteries: A first principles study. Phys. Chem. Chem. Phys. *25*, 26289–26297. https://doi.org/10.1039/d3cp02422a.
41. Song, D.-X., Ma, W.-G., and Zhang, X. (2020). Correlated migration of ions in a 2D heterostructure anode: Guaranteeing a low barrier for a high site occupancy. J. Mater. Chem. A *8*, 17463–17470. https://doi.org/10.1039/d0ta05595f.
42. Gavali, D.S., Kawazoe, Y., and Thapa, R. (2022). First-principles identification of interface effect on Li storage capacity of C_3N/graphene multilayer heterostructure. J. Colloid Interface Sci. *610*, 80–88. https://doi.org/10.1016/j.jcis.2021.12.052.
43. Chen, L., Yang, M., Kong, F., Guo, J., Shu, H., and Dai, J. (2022). Metallic penta-Graphene/penta-BN_2 heterostructure with high specific capacity: A novel application platform for Li/Na-ion batteries. J. Alloys Compd. *901*, 163538. https://doi.org/10.1016/j.jallcom.2021.163538.
44. Gavali, D.S., and Thapa, R. (2023). Identification of borophosphene/graphene heterostructure as anode for Li-ion batteries and its origin. J. Power Sources *566*, 232947. https://doi.org/10.1016/j.jpowsour.2023.232947.
45. Nair, A.K., Da Silva, C.M., and Amon, C.H. (2023). Enhanced alkali-ion adsorption in strongly bonded two-dimensional TiS_2/MoS_2 van der Waals heterostructures. J. Phys. Chem. C *127*, 9541–9553. https://doi.org/10.1021/acs.jpcc.3c01819.
46. Wang, T., Li, C., Xia, C., Yin, L., An, Y., Wei, S., and Dai, X. (2020). Silicene/BN vdW heterostructure as an ultrafast ion diffusion anode material for Na-ion battery. Phys. E Low Dimens. Syst. Nanostruct. *122*, 114146. https://doi.org/10.1016/j.physe.2020.114146.
47. Liu, H., Huang, Z., Wu, G., Wu, Y., Yuan, G., He, C., Qi, X., and Zhong, J. (2018). A novel WS_2/$NbSe_2$ vdW heterostructure as an ultrafast charging and discharging anode material for lithium-ion batteries. J. Mater. Chem. A *6*, 17040–17048. https://doi.org/10.1039/c8ta05531a.
48. Khan, M.I., Majid, A., Ashraf, N., and Ullah, I. (2020). A DFT study on a borophene/boron nitride interface for its application as an electrode. Phys. Chem. Chem. Phys. *22*, 3304–3313. https://doi.org/10.1039/c9cp06626h.
49. Zhen, M., Wang, J., Guo, S.-Q., and Shen, B. (2019). Vertically aligned nanosheets with MoS_2/N-doped-carbon interfaces enhance lithium-ion storage. Appl. Surf. Sci. *487*, 285–294. https://doi.org/10.1016/j.apsusc.2019.05.110.
50. Ma, J., Fu, J., Niu, M., and Quhe, R. (2019). MoO_2 and graphene heterostructure as promising flexible anodes for lithium-ion batteries. Carbon *147*, 357–363. https://doi.org/10.1016/j.carbon.2019.03.006.
51. Liu, B., Gao, T., Liao, P., Wen, Y., Yao, M., Shi, S., and Zhang, W. (2021). Metallic VS_2/graphene heterostructure as an ultra-high rate and high-specific capacity anode material for Li/Na-ion batteries. Phys. Chem. Chem. Phys. *23*, 18784–18793. https://doi.org/10.1039/d1cp02243a.
52. Samad, A., Noor-A-Alam, M., and Shin, Y.-H. (2016). First principles study of a SnS_2/graphene heterostructure: a promising anode material for rechargeable Na ion batteries. J. Mater. Chem. A *4*, 14316–14323. https://doi.org/10.1039/c6ta05739j.
53. Aierken, Y., Sevik, C., Gulseren, O., Peeters, F.M., and Cakir, D. (2018). MXenes/graphene heterostructures for Li battery applications: A first principles study. J. Mater. Chem. A *6*, 2337–2345. https://doi.org/10.1039/c7ta09001c.
54. Xie, X., Makaryan, T., Zhao, M., Van Aken, K.L., Gogotsi, Y., and Wang, G. (2016). MoS_2 nanosheets vertically aligned on carbon paper: A freestanding electrode for highly reversible sodium-ion batteries. Adv. Energy Mater. *6*, 1502161. https://doi.org/10.1002/aenm.201502161.
55. Tian, B., Tang, W., Leng, K., Chen, Z., Tan, S.J.R., Peng, C., Ning, G.-H., Fu, W., Su, C., Zheng, G.W., and Loh, K.P. (2017). Phase transformations in TiS_2 during K intercalation. ACS Energy Lett. *2*, 1835–1840. https://doi.org/10.1021/acsenergylett.7b00529.
56. Linganay, J.B.D., and Putungan, D.B. (2022). Adsorption and diffusion properties of calcium ions at the van der Waals interface of $NbSe_2$-graphene 2D heterostructure for multivalent battery applications: Density

functional theory calculations. Mater. Res. Express *9*, 095506. https://doi.org/10.1088/2053-1591/ac92c8.

57. Bediako, D.K., Rezaee, M., Yoo, H., Larson, D.T., Zhao, S.Y.F., Taniguchi, T., Watanabe, K., Brower-Thomas, T.L., Kaxiras, E., and Kim, P. (2018). Heterointerface effects in the electrointercalation of van der Waals heterostructures. Nature *558*, 425–429. https://doi.org/10.1038/s41586-018-0205-0.
58. Li, Y., Wu, W., and Ma, F. (2019). Blue phosphorene/graphene heterostructure as a promising anode for lithium-ion batteries: A firstprinciples study with vibrational analysis techniques. J. Mater. Chem. A *7*, 611–620. https://doi.org/10.1039/c8ta09423c.
59. Pomerantseva, E., and Gogotsi, Y. (2017). Two-dimensional heterostructures for energy storage. Nat. Energy *2*, 17089. https://doi.org/10.1038/nenergy.2017.89.
60. Wu, Y., and Yu, Y. (2019). 2D material as anode for sodium ion batteries: Recent progress and perspectives. Energy Stor. Mater. *16*, 323–343. https://doi.org/10.1016/j.ensm.2018.05.026.
61. Demiroglu, I., Peeters, F.M., Gülseren, O., Çakır, D., and Sevik, C. (2019). Alkali metal intercalation in MXene/Graphene heterostructures: A new platform for ion battery applications. J. Phys. Chem. Lett. *10*, 727–734. https://doi.org/10.1021/acs.jpclett.8b03056.
62. Samad, A., and Shin, Y.-H. (2017). MoS_2@VS_2 nanocomposite as a superior hybrid anode material. ACS Appl. Mater. Interfaces *9*, 29942–29949. https://doi.org/10.1021/acsami.7b07161.
63. Guo, G.-C., Wang, R.-Z., Ming, B.-M., Wang, C., Luo, S.-W., Zhang, M., and Yan, H. (2019). C_3N/phosphorene heterostructure: A promising anode material in lithium-ion batteries. J. Mater. Chem. A *7*, 2106–2113. https://doi.org/10.1039/c8ta10972a.
64. Xiang, P., Chen, X., Liu, J., Xiao, B., and Yang, L. (2018). Borophene as conductive additive to boost the performance of MoS_2-based anode materials. J. Phys. Chem. C *122*, 9302–9311. https://doi.org/10.1021/acs.jpcc.8b00768.
65. Yu, J., Zhou, M., Yang, M., Yang, Q., Zhang, Z., and Zhang, Y. (2020). High-performance borophene/graphene heterostructure anode of lithium-ion batteries achieved via controlled interlayer spacing. ACS Appl. Energy Mater. *3*, 11699–11705. https://doi.org/10.1021/acsaem.0c01808.
66. Lu, Y.-M., Yang, J.-L., Zhao, S.-X., Zeng, X.-T., Yu, L.-Q., and Huang, C. (2021). Double role of CoO Co_4N hetero-nanocages as sulfur host for lithium-sulfur batteries. J. Materiomics *7*, 1301–1308. https://doi.org/10.1016/j.jmat.2021.02.019.
67. Dai, H., Zhao, X., Xu, H., Yang, J., Zhou, J., Chen, Q., and Sun, G. (2022). Design of vertically aligned two-dimensional heterostructures of rigid $Ti_3C_2T_X$ MXene and pliable vanadium pentoxide for efficient lithium ion storage. ACS Nano *16*, 5556–5565. https://doi.org/10.1021/acsnano.1c10212.
68. Yan, P., Ji, L., Liu, X., Guan, Q., Guo, J., Shen, Y., Zhang, H., Wei, W., Cui, X., and Xu, Q. (2021). 2D amorphous-MoO_{3-x}@Ti_3C_2-MXene non-van der Waals heterostructures as anode materials for lithium-ion batteries. Nano Energy *86*, 106139. https://doi.org/10.1016/j.nanoen.2021.106139.
69. Guo, W., Jiang, J., Zhou, Y., Cheng, Z., Yang, J., Li, S., and Xu, Q. (2022). Supercritical CO_2-built 2D Fe_xN@FeOOH heterostructures for sustainable sodium ion battery. Energy Fuels *36*, 7194–7199. https://doi.org/10.1021/acs.energyfuels.2c01445.
70. Wu, Y., Wei, W., Ding, T., Chen, S., Zhai, R., and Bai, C. (2021). Modulating a 2D heterointerface with g-C_3N_4 mesh layers: A suitable hetero-layered architecture for high-power and long-life energy storage. J. Mater. Chem. A *9*, 7791–7806. https://doi.org/10.1039/d0ta12497d.
71. Zhang, Y., Qin, J., Batmunkh, M., Li, W., Fu, H., Wang, L., Al-Mamun, M., Qi, D., Liu, P., Zhang, S., and Zhong, Y.L. (2022). Scalable spray drying production of amorphous V_2O_5-EGO 2D heterostructured xerogels for high-rate and high-capacity aqueous zinc ion batteries. Small *18*, 2105761. https://doi.org/10.1002/smll.202105761.
72. Liu, C., Xu, W., Mei, C., Li, M.-C., Xu, X., and Wu, Q. (2021). Highly stable $H_2V_3O_8$/MXene cathode for Zn-ion batteries with superior rate performance and long lifespan. Chem. Eng. J. *405*, 126737. https://doi.org/10.1016/j.cej.2020.126737.
73. Wang, X., Li, Y., Das, P., Zheng, S., Zhou, F., and Wu, Z.-S. (2020). Layer-by-layer stacked amorphous V_2O_5/Graphene 2D heterostructures with strong-coupling effect for high-capacity aqueous zinc-ion batteries with ultra-long cycle life. Energy Stor. Mater. *31*, 156–163. https://doi.org/10.1016/j.ensm.2020.06.010.
74. Xu, M., Wu, T., Qi, J., Zhou, D., and Xiao, Z. (2021). V_2C/VO_2 nanoribbon intertwined nanosheet dual heterostructure for highly flexible and robust lithium-sulfur batteries. J. Mater. Chem. A *9*, 21429–21439. https://doi.org/10.1039/d1ta05693j.
75. Xu, H., Zhang, H., Wang, Y., Tang, C., Xiao, T., Xu, Z., Li, H., Xu, F., and Mai, Y. (2023). Two-dimensional sandwich-like MXene-conductive polymer nanocomposite with in-plane cylindrical mesopores for long cycling lithium-sulfur batteries. 2D Mater. *10*, 024006. https://doi.org/10.1088/2053-1583/acbec4.
76. Xiong, P., Zhang, F., Zhang, X., Wang, S., Liu, H., Sun, B., Zhang, J., Sun, Y., Ma, R., Bando, Y., et al. (2020). Strain engineering of two-dimensional multilayered heterostructures for beyond-lithium-based rechargeable batteries. Nat. Commun. *11*, 3297. https://doi.org/10.1038/s41467-020-17014-w.
77. Choi, I.Y., Jo, C., Lim, W.-G., Han, J.-C., Chae, B.-G., Park, C.G., Lee, J., and Kim, J.K. (2019). Amorphous tin oxide nanohelix structure based electrode for highly reversible Na-ion batteries. ACS Nano *13*, 6513–6521. https://doi.org/10.1021/acsnano.8b09773.
78. Ma, M., Zhang, S., Wang, L., Yao, Y., Shao, R., Shen, L., Yu, L., Dai, J., Jiang, Y., Cheng, X., et al. (2021). Harnessing the volume expansion of MoS_3 anode by structure engineering to achieve high performance beyond lithium-based rechargeable batteries. Adv. Mater. *33*, 2106232. https://doi.org/10.1002/adma.202106232.
79. Liu, Q., Hu, Z., Li, W., Zou, C., Jin, H., Wang, S., Chou, S., and Dou, S.-X. (2021). Sodium transition metal oxides: the preferred cathode choice for future sodium-ion batteries? Energy Environ. Sci. *14*, 158–179. https://doi.org/10.1039/d0ee02997a.
80. Tan, C., Cao, X., Wu, X.-J., He, Q., Yang, J., Zhang, X., Chen, J., Zhao, W., Han, S., Nam, G.-H., et al. (2017). Recent advances in ultrathin two-dimensional nanomaterials. Chem. Rev. *117*, 6225–6331. https://doi.org/10.1021/acs.chemrev.6b00558.
81. Das, P., Fu, Q., Bao, X., and Wu, Z.-S. (2018). Recent advances in the preparation, characterization, and applications of two-dimensional heterostructures for energy storage and conversion. J. Mater. Chem. A *6*, 21747–21784. https://doi.org/10.1039/c8ta04618b.
82. Wang, W., Hu, L., Li, L., Liu, C., Liu, X., Wang, H., and Zhai, G. (2023). Constructing a rapid ion and electron migration channels in $MoSe_2$/$SnSe_2$@C 2D heterostructures for high-efficiency sodium-ion half/full batteries. Electrochim. Acta *449*, 142239. https://doi.org/10.1016/j.electacta.2023.142239.
83. Zou, P., Zhang, R., Yao, L., Qin, J., Kisslinger, K., Zhuang, H., and Xin, H.L. (2021). Ultrahigh-rate and long-life zinc-metal anodes enabled by self-accelerated cation migration. Adv. Energy Mater. *11*, 2100982. https://doi.org/10.1002/aenm.202100982.
84. Liu, Y., and Wu, X. (2021). Review of vanadium-based electrode materials for rechargeable aqueous zinc ion batteries. J. Energy Chem. *56*, 223–237. https://doi.org/10.1016/j.jechem.2020.08.016.
85. Zheng, S., Zhao, W., Chen, J., Zhao, X., Pan, Z., and Yang, X. (2023). 2D Materials boost advanced Zn anodes: Principles, advances, and challenges. Nano-Micro Lett. *15*, 46. https://doi.org/10.1007/s40820-023-01021-9.
86. Xu, W., Zhang, M., Dong, Y., and Zhao, J. (2022). Two-dimensional materials for dendrite-free zinc metal anodes in aqueous zinc batteries. Batteries *8*, 293. https://doi.org/10.3390/batteries8120293.
87. Kundu, D., Adams, B.D., Duffort, V., Vajargah, S.H., and Nazar, L.F. (2016). A high-capacity and long-life aqueous rechargeable zinc battery using a metal oxide intercalation cathode. Nat. Energy *1*, 16119. https://doi.org/10.1038/nenergy.2016.119.
88. Liu, C., Neale, Z., Zheng, J., Jia, X., Huang, J., Yan, M., Tian, M., Wang, M., Yang, J., and Cao, G. (2019). Expanded hydrated vanadate for high-performance aqueous zinc-ion batteries. Energy Environ. Sci. *12*, 2273–2285. https://doi.org/10.1039/c9ee00956f.
89. Liu, X., Jin, Y., Wang, H., Yang, X., Zhang, P., Wang, K., and Jiang, J. (2022). *In situ* growth of covalent organic framework nanosheets on graphene as the cathode for long-life high-capacity lithium-ion batteries. Adv. Mater. *34*, 2203605. https://doi.org/10.1002/adma.202203605.
90. Qian, J., Xing, Y., Yang, Y., Li, Y., Yu, K., Li, W., Zhao, T., Ye, Y., Li, L., Wu, F., and Chen, R. (2021). Enhanced electrochemical kinetics with highly dispersed conductive and electrocatalytic mediators for lithium-sulfur batteries. Adv. Mater. *33*, 2100810. https://doi.org/10.1002/adma.202100810.
91. Peng, L., Wei, Z., Wan, C., Li, J., Chen, Z., Zhu, D., Baumann, D., Liu, H., Allen, C.S., Xu, X., et al. (2020). A fundamental look at electrocatalytic sulfur reduction reaction. Nat. Catal. *3*, 762–770. https://doi.org/10.1038/s41929-020-0498-x.
92. Li, S., Zhang, W., Zheng, J., Lv, M., Song, H., and Du, L. (2021). Inhibition of polysulfide shuttles in Li-S batteries: modified separators and solid-state electrolytes. Adv. Energy Mater. *11*, 2000779. https://doi.org/10.1002/aenm.202000779.
93. Wu, S., Li, X., Zhang, Y., Guan, Q., Wang, J., Shen, C., Lin, H., Wang, J., Wang, Y., Zhan, L., and Ling, L. (2023). Interface engineering of MXene-based heterostructures for lithium-sulfur batteries. Nano Res. *16*, 9158–9178. https://doi.org/10.1007/s12274-023-5532-2.

94. Long, X., Luo, Z.-H., Zhou, W.-H., Zhu, S.-K., Song, Y., Li, H., Geng, C.-N., Shi, B., Han, Z.-Y., Zhou, G.-M., et al. (2022). Two-dimensional montmorillonite-based heterostructure for high-rate and long-life lithium-sulfur batteries. Energy Stor. Mater. *52*, 120–129. https://doi.org/10.1016/j.ensm.2022.07.041.

95. Zhang, G., Zhou, C., Long, J., Li, Y., Lv, L., Yan, K., Chen, X., Dong, C., Xu, X., and Mai, L. (2023). Bottom-up synthesis of 2D heterostructures enables effective polysulfides inhibition and conversion. Nano Res. *16*, 8488–8496. https://doi.org/10.1007/s12274-023-5535-z.

96. Xu, S.-M., Liang, X., Wu, X.-Y., Zhao, S.-L., Chen, J., Wang, K.-X., and Chen, J.-S. (2019). Multistaged discharge constructing heterostructure with enhanced solid-solution behavior for long-life lithium-oxygen batteries. Nat. Commun. *10*, 5810. https://doi.org/10.1038/s41467-019-13712-2.

97. Wang, P., Ren, Y., Wang, R., Zhang, P., Ding, M., Li, C., Zhao, D., Qian, Z., Zhang, Z., Zhang, L., and Yin, L. (2020). Atomically dispersed cobalt catalyst anchored on nitrogen-doped carbon nanosheets for lithium-oxygen batteries. Nat. Commun. *11*, 1576. https://doi.org/10.1038/s41467-020-15416-4.

98. Gong, H., Wang, T., Chang, K., Li, P., Liu, L., Yu, X., Gao, B., Xue, H., Ma, R., He, J., and Ye, J. (2022). Revealing the illumination effect on the discharge products in high-performance Li–O_2 batteries with heterostructured photocatalysts. Carbon Energy *4*, 1169–1181. https://doi.org/10.1002/cey2.208.

99. Ye, X., Han, Z., Yan, Q., Feng, J.-J., Mei, L.-P., Zhang, L., and Wang, A.-J. (2021). CoNi/MoC nanoparticles entrapped into N, P-codoped carbon nanotubes-on-nanosheets: A synergy of 1D@2D heterostructures with multiple active sites for rechargeable Zn-air battery. J. Power Sources *506*, 230225. https://doi.org/10.1016/j.jpowsour.2021.230225.